석사 학위논문
Master's Thesis

3차원 빔 해석에서의 내부 슬립 모델링

Modeling Interlayer Slips in 3D Beam Analysis

김 효 진 (金 效 津 Kim, Hyo-Jin)
기계항공시스템공학부 해양시스템전공
School of Mechanical, Aerospace and Systems Engineering,
Division of Ocean Systems Engineering

KAIST

2015

3 차원 빔 해석에서의 내부 슬립 모델링

Modeling Interlayer Slips in 3D Beam Analysis

Modeling Interlayer Slips in 3D Beam Analysis

Advisor : Professor Lee, Phill-Seung

by

Kim, Hyo-Jin
School of Mechanical, Aerospace and Systems Engineering,
Division of Ocean Systems Engineering

KAIST

A thesis submitted to the faculty of KAIST in partial fulfillment of the requirements for the degree of Master of Science and Engineering in the School of Mechanical, Aerospace and Systems Engineering, Division of Ocean Systems Engineering. The study was conducted in accordance with Code of Research Ethics[1]

2014. 12. 19

Approved by

Professor Lee, Phill-Seung

[1] Declaration of Ethical Conduct in Research: I, as a graduate student of KAIST, hereby declare that I have not committed any acts that may damage the credibility of my research. These include, but are not limited to: falsification, thesis written by someone else, distortion of research findings or plagiarism. I affirm that my thesis contains honest conclusions based on my own careful research under the guidance of my thesis advisor.

3 차원 빔 해석에서의 내부 슬립 모델링

김 효 진

위 논문은 한국과학기술원 석사학위논문으로
학위논문심사위원회에서 심사 통과하였음.

2014 년 12 월 19 일

심사위원장 이 필 승 (인)

심사위원 정 현 (인)

심사위원 조 연 우 (인)

MOSE
20133215

김 효 진. Kim, Hyo Jin. Modeling Interlayer Slips in 3D Beam Analysis. 3차원 빔 해석에서의 내부 슬립 모델링. School of Mechanical Aerospace and Systems Engineering, Division of Ocean Systems Engineering. 2015. 57p. Advisor Prof. Lee, Phill-seung.

ABSTRACT

Multi-layered composite beams, which consist of multiple layers with different material are commonly used in various engineering fields to obtain enhanced structural property. However, complete shear connection between the layers can hardly be achieved in practice and it gives rise to partial interaction between the layers. The partial interaction in the multi-layered composite beam induces interlayer slips between the layers and it results in a decrease in strength and an increase in deflection. Thus, the partial interaction effect between the layers and the resulting interlayer slips should be taken into account for optimal design and accurate analysis of the actual behavior of the multi-layered structures.

In spite of many analysis of two-layer and three-layer composite beams with deformable shear connections, the researches about general multi-layered structures have been very rarely discussed and most of the researches are limited to only two-dimensional loading condition. In order to fulfill the needs for more accurate evaluation of the actual structure behavior, the further study about the three-dimensional model for general multi-layered beam structure is necessary.

In the present research, the beam finite element which is applicable to the three-dimensional analysis of the multi-layered composite beam structures was introduced. Instead of modeling the each layer of the beam, the beam structure was regarded as an association of the sub-beams including slip modes. Consequently, the displacement field of the multi-layered composite beam was decomposed into the displacements of the associated sub-beams represented by a single beam element and the slip displacements modeled by slip modulus and slip modes that composed of the bending slip modes and axial slip modes. Load-slip relation is assumed to be linear elastic behavior with the constant slip modulus. Since the total slip displacements are represented by slip modes with the slip modulus, only two additional DOFs are required for the two-dimensional analysis and it can be easily extended to the three-dimensional problems by inserting another slip DOF corresponding to the extended dimension.

The main advantage of the present beam model is that any multi-layered beam can be modeled by a single beam and slip modes. Therefore, the present beam element enables straightforward modeling of the multi-layered composite beam with relatively small number of DOFs. Also, three-dimensional analysis can be easily performed without complicated modeling procedure by applying additional slip mode with corresponding slip DOF.

In order to verify the present beam model, several numerical studies are performed. Firstly, the present beam model is compared to the conventional one to demonstrate the influence of the slip modulus on the partial interaction effect. Secondly, the numerical examples discussed by other authors are examined. Lastly, extension to the three-dimensional problem is introduced

Keywords: Multi-layered beam, Composite beam, Interlayer slip, Partial interaction, Shear connection

Table of Contents

List of Tables

List of Figures

Chapter 1. Introduction

1.1 Research Background and Motivation

Multi-layered composite beams, which consist of multiple layers with different materials are commonly used in various engineering fields to obtain enhanced structural properties such as high strength, high performance, light weight, low cost, etc. As typical examples, steel-concrete composite beam and layered timber beam have been widely used for buildings and bridges construction. Normally, each component of the multi-layered composite beam is connected by shear connections that transfer shear stress to each other. Rigid shear connection which performs full shear connection between the components enables desired behavior of multi-layered composite beam. However, because of the finite stiffness of the shear connection complete shear interaction can hardly be achieved in practice and it give rise to partial interaction between the layers. Therefore, partial interaction due to the incomplete shear connection exhibits in most of the composite beams.

Partial interaction of the multi-layered composite beam induces interlayer slip between the layers and it results in a decrease in strength and an increase in deflection. Thus, the partial interaction effect between the layers and the interlayer slips should be taken into account for optimal design and accurate analysis of the actual behavior of the multi-layered structures. Consequently, many numerical and analytical researches have been proposed to investigate aforementioned phenomenon.

Analytical formulation for two-layer partially connected composite beams with linear shear connection stiffness was originally developed based on the Euler-Bernoulli beam theory by Newmark et al. [6] in the early 50s. Afterward, Girhammar and Gopu [7] presented the differential equations of partially connected composite beam with their exact solutions and compared first and second order analyses and Goodman and Popov [8] extended Newmark model to analysis of a three-layered composite beam. Since then, many analytical researches have been presented. Later on, shear deformation effect was considered according to the Timoshenko beam theory for detailed analysis of the partially connected composite beams. Schnabl et al. [9] and Xu and Wu [10] presented analytical models for two-layer and three-layer composite beams with deformable shear connectors. However, the closed-form solutions for general problems can hardly be obtained.

Alternatively, numerical methods have been developed for more complicated problems, mostly based on the finite element analysis. Ranzi et al. [11] proposed a direct stiffness FE formulation based on the exact expressions and Battini et al. [12] presented exact FE formulations for nonlinear behavior of partially connected composite beam according to Euler-Bernoulli beam theory. Also, Nguyen et al. [13] developed an exact finite element model for composite beams with partial interaction by employing the Timoshenko beam theory. In addition, strain-based, force-based and mixed FE model was developed. Schnabl et al. [14] proposed two-layer planar composite beam element based on Timoshenko beam theory and Cˇas et al. [15] presented FE formulation for composite planar frame with nonlinear geometry.

In spite of many analysis of two-layer and three-layer composite beam with shear connections, the researches about general multi-layered structures have been very rarely discussed. To cite a few, Sousa Jr. and Silva [16] developed the analytical and numerical model for multi-layered composite beam employing zero-thickness interface elements. Also, Davi et al. [17] presented analytical model for multi-layered beam subjected to axial, bending and shear end load. However, most of the researches about multi-layered composite beam are limited to only two-dimensional loading conditions. In order to fulfill the needs for more accurate evaluation of the actual structure behavior of multi-layered composite beam with partial interaction effects, it is apparent that the further study about the three-dimensional model for general multi-layered beam structure is necessary.

1.2 Research Purpose

Generally, it is complicated to obtain the solution for the structural systems composed of multiple layers that connected by deformable shear connections. As the number of layers increases, the solution procedures become more complex due to the large number of unknowns which depend on the number of sub-elements used to discretize cross-section geometry. Thus, existing FE model can hardly be applied to multi-layered composite beam structures with a number of interlayers and also, analytical solution procedures are too complex to be employed. In three-dimensional problems, the behavior of the multi-layered composite beam structures become more complicated and it is hard to be analyzed by two-dimensional FE model. In addition, the FE models that enable three-dimensional analysis of the partial interactions and interlayer slips of the multi-layered composite beams have been rarely presented.

The purpose of this research is to develop finite element formulation which is applicable to the multi-layered composite beam structures with relatively small number of DOFs and is easily extended to the three-dimensional model. To this end, the multi-layered composite beam structure was regarded as an association of the sub-beams rather than as respective components in the present model. The displacement fields of the multi-layered composite beam was decomposed into the displacements of the associated sub-beams which can be represented by nodal displacements of beam nodes in single beam element and the slip displacements which can be modeled by slip modes and slip modulus. The slip modes indicate the whole slip displacements of the multi-layered structure including relative horizontal displacements of the each layer with no partial interactions and the slip modulus is employed for the partial interaction effects at the interlayers. The slip modes are composed of the bending slip modes and axial slip modes, and each slip modes can be modeled by slip function with 1 DOF at the beam nodes. The partial interaction effects at the interlayers are modeled by the slip stiffness matrix corresponding slip DOFs. Because the total slip displacements are represented by the slip modes, only two additional DOFs at each beam node are required for the two-dimensional analysis procedure of the present model. Also, it is straightforward to extend the present model to a more general three-dimensional problems by applying another additional slip mode corresponding to extended dimension.

1.3 Organization of the Thesis

- In chapter 2, basic assumptions of the present slip model were introduced. Then, the concept of slip modes, which is a key idea of the present model is explained in detail. Also, load-slip relation and constant slip modulus for modeling partial interaction effect between the layers were explained.
- In chapter 3, formulation of continuum mechanics based beam element was briefly introduced. Then, enriched beam formulation including slip modes with corresponding slip DOFs was derived. Also, calculation procedure of bending slip function and axial slip function is explained in detail.
- In chapter 4, principle of virtual work was briefly reviewed and variational formulation of the present beam element was derived. Then, finite element formulations obtained based on the weak form were explained. For finite element analysis, linearized covariant Green-Lagrange strain was employed and standard numerical integration procedure was adopted.
- In chapter 5, several numerical examples were presented for the verification of the proposed beam model. The present beam model was compared with conventional one to verify the partial interaction effect. Also, numerical examples discussed in other literatures were examined. Lastly, extension to the three-dimensional problem was introduced.
- In chapter 6, conclusions of the present research and further studies were summarized briefly.

Chapter 2. Numerical Interlayer Slip Model

2.1. Basic assumption

Partial composite interaction due to the deformable shear connection induces interlayer slip, which is relative horizontal displacements between the adjacent layers. Normally, the vertical separations between the layers are often negligible and only relative displacements in horizontal directions are considered in multi - layered structures as shown in Figure 2.1

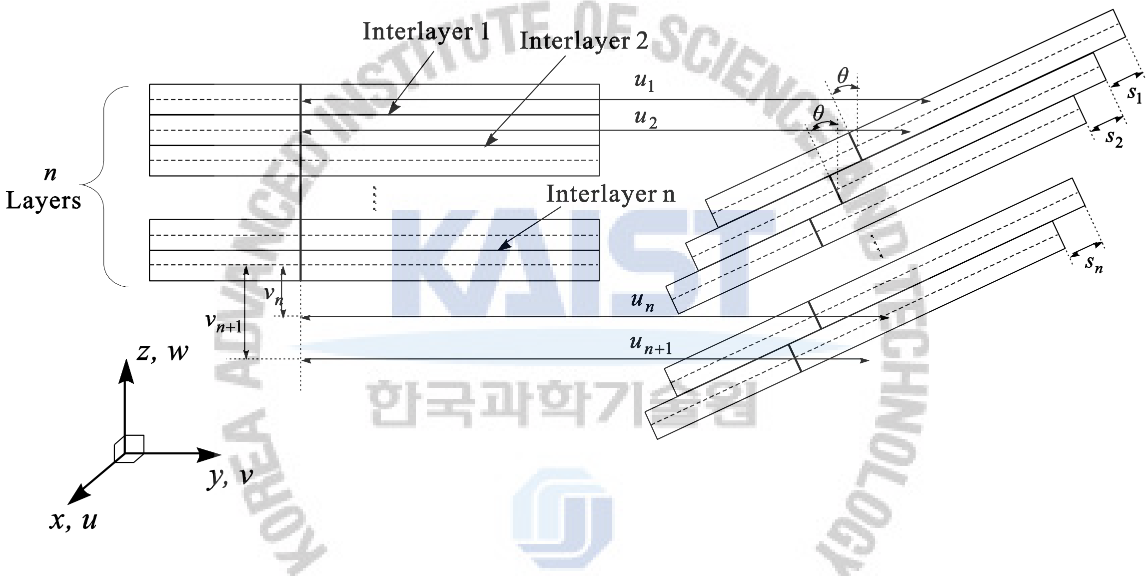

Figure 2.1 Relative horizontal displacements in n-layered multi-layered structure with no vertical separations.

In the present research, the behavior of the multi-layered composite beam structure is investigated and finite element formulation that can be easily applied to the three-dimensional problems with relatively small number of DOFs is presented. To this end, the multi-layered composite beam structure was regarded as an association of the sub-beams with no transvers separation. The basic assumptions for the presented slip model are explained as follows.

(a) The analysis of each sub-beam of multi-layered composite beam is carried out based on Timoshenko beam theory, which considers shear deformation effects.

(b) The relative horizontal displacements (interlayer slips) occur at the interface between the adjacent layers and vertical separations are neglected.

(c) The beams are subjected to transverse and axial loading. Applied axial loads are uniformly distributed at the cross-section.

(d) Each layer of the multi-layered composite beam is assumed to have same curvature.

(e) Linear elastic material behavior is assumed.

(f) Shear connections that located discretely at interlayers are regarded as continuous.

(g) The relation between slip load and slip displacement is linear elastic with a constant slip modulus K [N/m2].

2.2 Slip Modes

When multi-layered composite beam with deformable shear connections is loaded, incomplete interactions are caused according to the partial transfer of shear stresses at the interlayers and it leads to decrease in strength and an increase in deflection. As a consequence of the incomplete partial interactions due to the deformable shear connections, relative horizontal displacement, which is interlayer slip often develops as shown in Figure 2.2

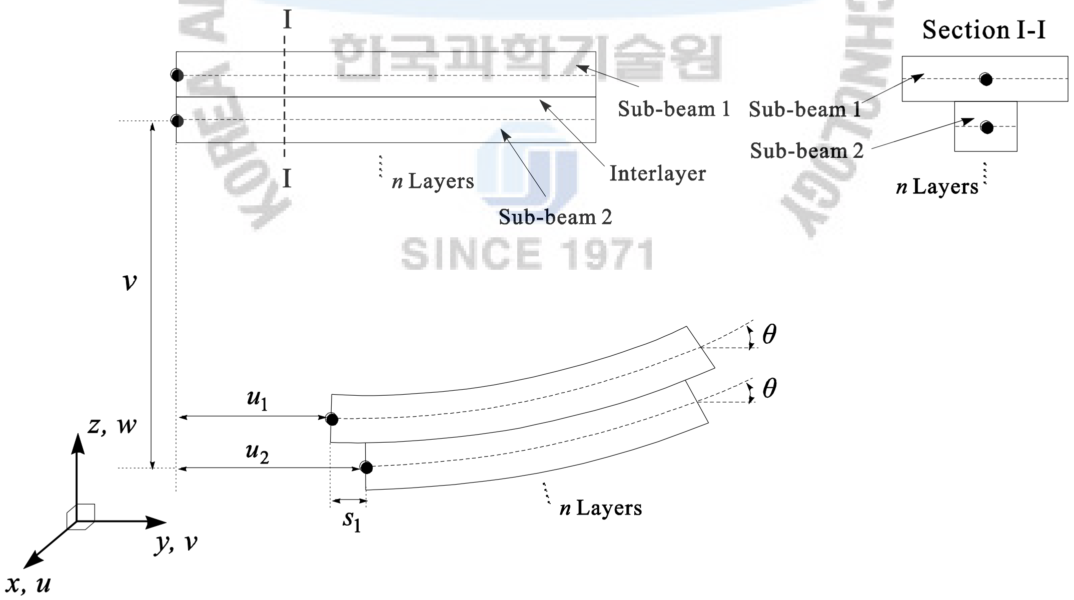

Figure 2.2 Deformed shape of the multi-layered composite beams with deformable shear connections with same rotation and curvature.

Based on the aforementioned assumptions, the curvature and axial strains at cross-section are expressed as follows.

$$\varepsilon_1 = \frac{\partial u_1}{\partial x},\ \ \varepsilon_2 = \frac{\partial u_2}{\partial x},\ \ \ldots\ ,\ \ \varepsilon_n = \frac{\partial u_n}{\partial x}$$

$$\kappa = \frac{\partial \theta}{\partial x} = \frac{\partial^2 \mathrm{v}}{\partial x^2} \tag{2-1}$$

where ε_m is the axial strain at the cross-section centroid of sub-beam m, v is the transverse displacement, θ is $\partial \mathrm{v}/\partial x$ and κ is the curvature.

In the present model, multi-layered composite beam structure was treated as an association of the sub-beams with slip displacement fields of each layers rather than as respective components. For this purpose, the displacement fields of the multi-layered composite beam was decomposed into the displacements of the associated sub-beams and slip displacements. The displacement fields of an association of the sub-beams can be represented by nodal displacements at beam nodes in a single beam that contains classical deformation modes. Meanwhile, the slip displacements are modeled by the slip modes, which are the additional individual modes at beam nodes and the slip modulus is employed for the partial interaction effect at the interlayer.

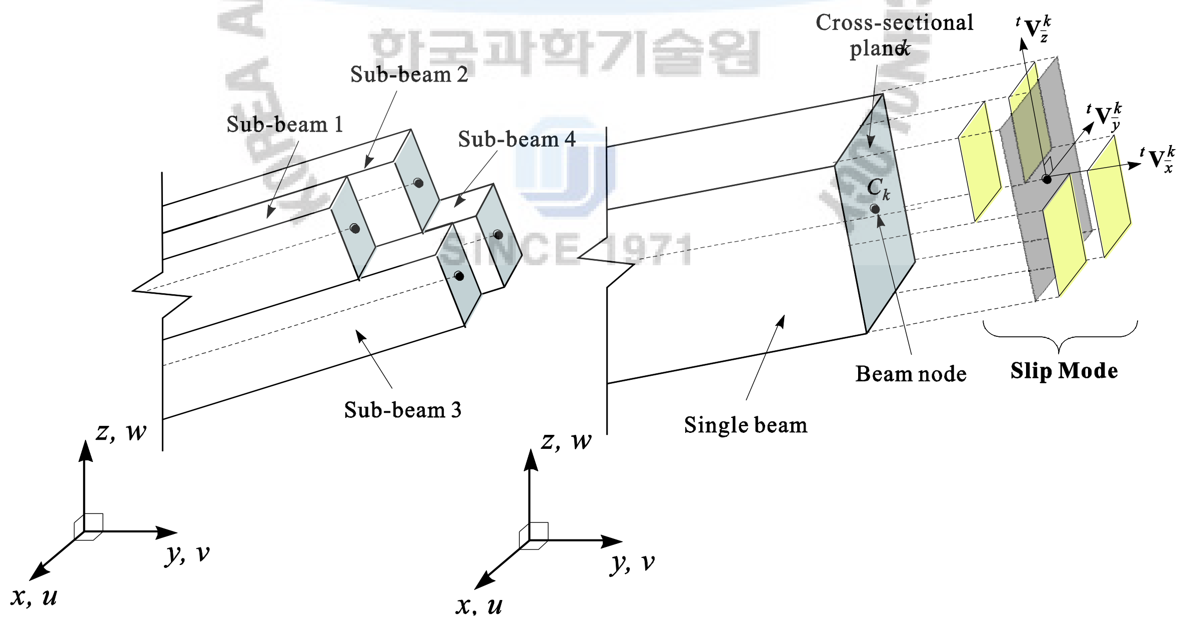

Figure 2.3(a) Interlayer slips in 4-layered multi-layered beam structures

Figure 2.3(b) Interlayer slips modeled by a single beam element with slip mode

The slip modes are individual modes that represent total interlayer slip displacements between the sub-beams under no partial interaction effect. The concept of the slip mode is briefly described in Figure 2.3(a) and Figure 2.3(b). Figure 2.3(a) shows interlayer slips in 4-layered beam structures. These interlayer slips can be modeled by the displacement fields of a single beam and slip mode at beam node as shown in Figure 2.3(b) where ${}^t\mathbf{V}_{\bar{z}}^k$ and ${}^t\mathbf{V}_{\bar{y}}^k$ denote the director vectors in the cross-sectional plane k at time t, which is normal to each other. The director vectors ${}^t\mathbf{V}_{\bar{z}}^k$ and ${}^t\mathbf{V}_{\bar{y}}^k$ and the origin C_k define the cross-sectional Cartesian coordinate system and ${}^t\mathbf{V}_{\bar{x}}^k$ denotes the interlayer slip direction calculated by ${}^t\mathbf{V}_{\bar{x}}^k = {}^t\mathbf{V}_{\bar{y}}^k \times {}^t\mathbf{V}_{\bar{z}}^k$. The slip modes are composed of the bending slip mode due to bending moments and axial slip mode due to axial loads.

2.2.1 Bending slip mode

The bending slip mode represents the slip displacement at the cross-section of the multi-layered composite beam subjected to the bending moments with no partial interactions. Because there is no composite interaction effect between the layers, each sub-beam has its own neutral axis and corresponding bending moments are produced as described in Figure 2.4.

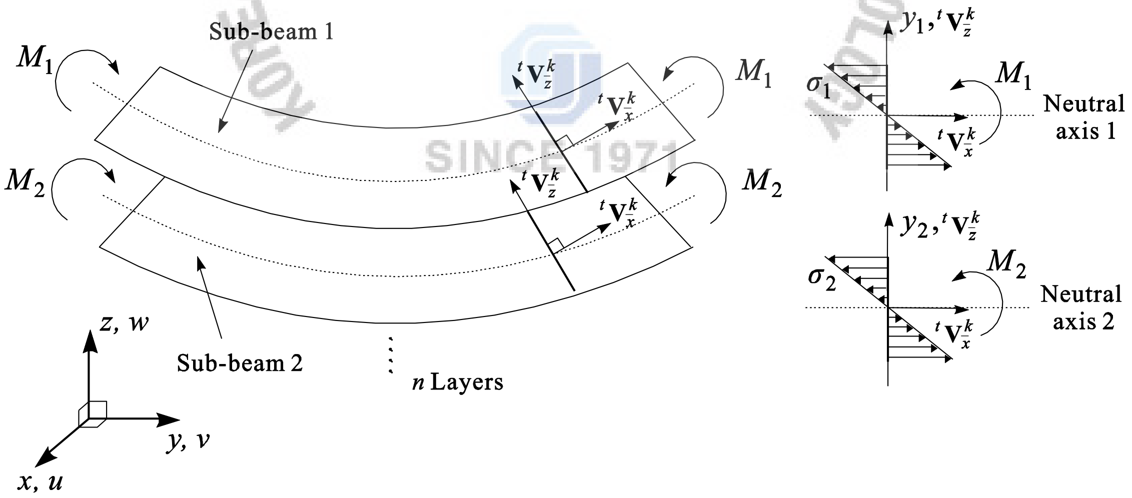

Figure 2.4 Bending moments and corresponding bending stresses in the cross-section of the multi-layered composite beam with no partial interaction.

If the positive bending moment is applied as shown in Figure 2.4, the lower part of the sub-beam 1 under the neutral axis 1 is subjected to the positive bending stresses where y_1 is negative. On the other hand, the upper part of the sub-beam 2 over the neutral axis 2 is subjected to the negative bending stresses where y_2 is positive. Therefore the relative horizontal displacement occurs at the interlayer between the sub-beam 1 and sub-beam 2 in ${}^{t}\mathbf{V}_{\bar{x}}^{k}$ direction.

Based on the assumption of the small deformation, each sub-beam has same curvature and rotation. According to this, the interlayer slip displacements in bending slip mode can be derived as below,

$$s_i^b = u_{i+1} - u_i + d_i \frac{\partial v}{\partial x} = d_i \theta, \quad i = 1, 2, \cdots, n-1, \tag{2-2}$$

where s_i^b is interlayer slips between the sub-beam $i+1$ and sub-beam i under pure bending condition, d_i is length between the centroid of sub-beam $i+1$ and the centroid of sub-beam i, θ is the rotation, and n is the number of sub-beams. Note that u_{i+1} and u_i are same under the pure bending condition. (Figure 2.5)

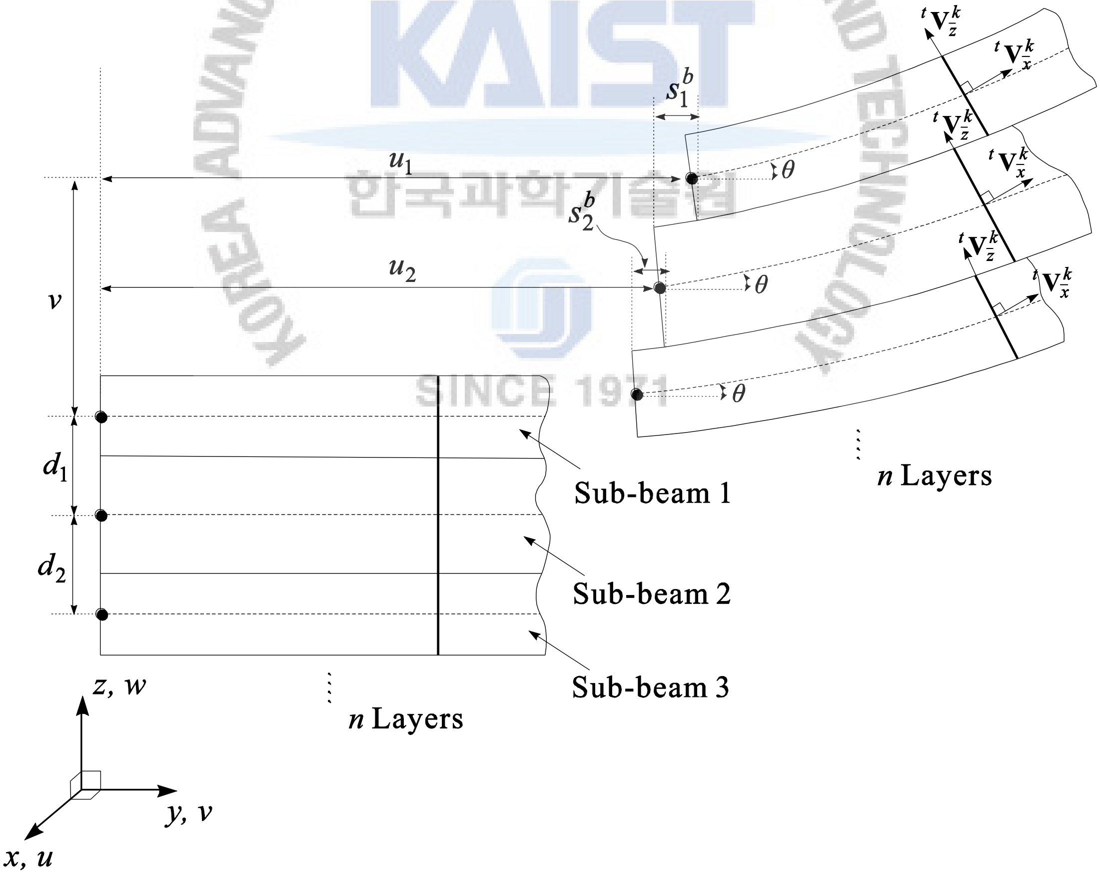

Figure 2.5 The displacements field of the multi-layered beam subjected to bending moments.

2.2.2 Axial slip mode

Similarly, when axial load is applied to the multi-layered composite beam with no partial interaction effect, slip displacements can be represented by axial slip modes. The slip displacements caused by axial loading are observed with the different material property of the each layers as shown in Figure 2.6 since the present model assumed uniform distribution of the axial loading in the cross section of the multi-layered composite beams.

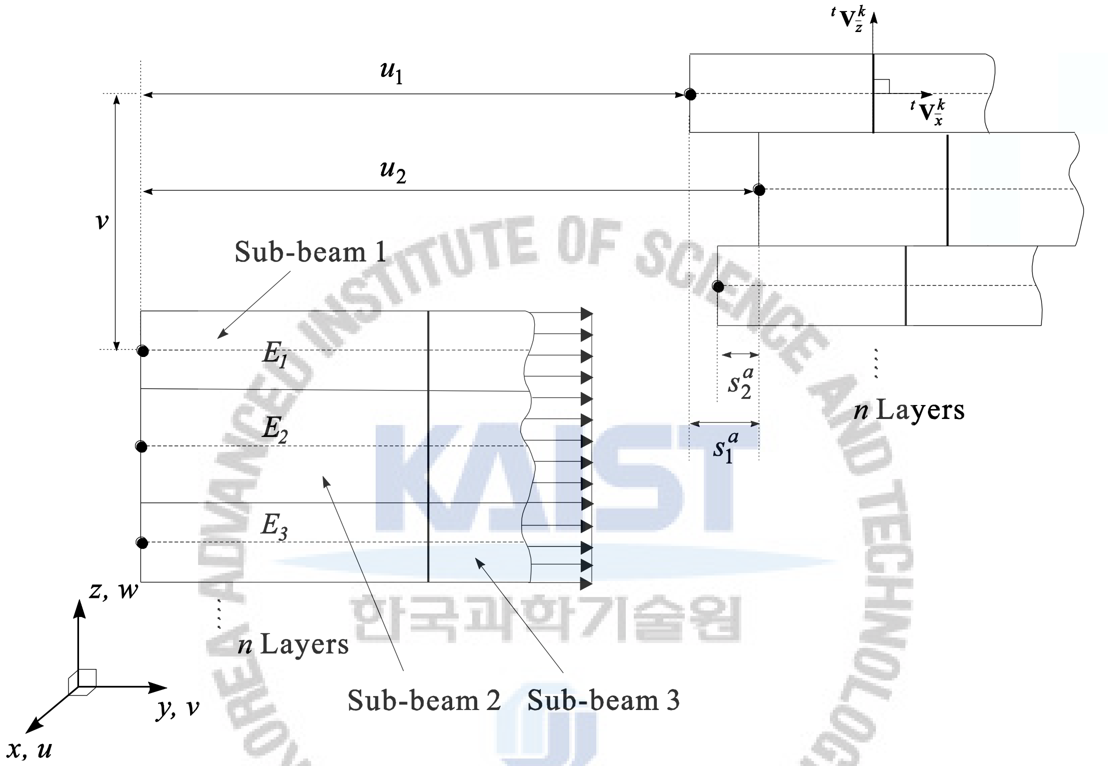

Figure 2.6 The displacements field of the multi-layered beam under uniformly distribution of axial loading condition

Consequently, the interlayer slips in axial slip mode, which is relative horizontal displacements between the layers under uniformly distributed axial loading condition is obtained by difference of the horizontal displacement between adjacent layers as below.

$$s_i^a = u_{i+1} - u_i = \frac{P_{i+1}L}{E_{i+1}A_{i+1}} - \frac{P_iL}{E_iA_i} = \frac{P_0L}{A_0}\left(\frac{1}{E_{i+1}} - \frac{1}{E_i}\right), \quad i = 1,2,\cdots,n-1 \tag{2-3}$$

where s_i^a is interlayer slip displacements between the sub-beam $i+1$ and sub-beam i under uniform axial loading distribution, E_i is Young's modulus of the sub-beam i, A_i is cross-section area of the sub-beam i, P_i is resultant axial force of the sub-beam i, L is the length of the beam and n is the number of sub-beams. According to the assumption of uniform axial loading distribution, each sub-beam is subjected to uniform axial stress P_0/A_0. Note that the interlayer slip displacement between the sub-beam $i+1$ and sub-beam i under uniform axial loading distribution is proportional to $(1/E_{i+1} - 1/E_i)$.

2.3 Slip Function

The slip modes composed of bending slip mode and axial slip mode are modeled by slip functions with slip degree of freedoms (DOFs) in beam formulation. Each slip mode can be represented by corresponding slip functions with slip DOF individually. The slip function is the step function defined over the cross-section of the beam, in which the value of the slip functions indicates the extent of deformation in ${}^t\mathbf{V}_{\bar{x}}^k$ direction. The concept of the slip function is described briefly in Figure 2.7.

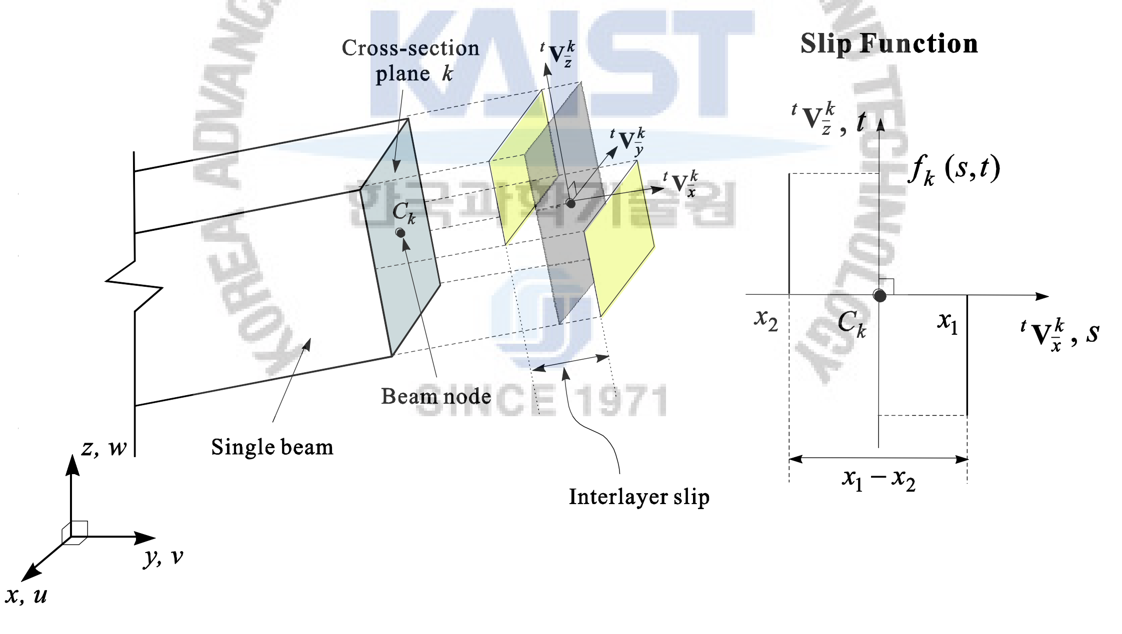

Figure 2.7 The concept of slip function on the cross-sectional plane k in the two-layer beam with deformable shear connection

Since the jumps at the discontinuity point of the slip function indicates the extent of the interlayer slip displacements at the sub-beams, the slip modes can be obtained by the multiplication of slip function and slip DOF. The calculation procedures for both bending slip function and axial slip function are introduced specifically in section 3.2.2.

2.4 Slip Modulus

The function of shear connections is to transfer the shear force between the layers and to prevent the vertical separation of the components of the multi-layered structure. Rigid connectors provide full shear connection and enables perfect composite action between the components of the multi-layered composite structure. On the other hand, flexible connectors such as bolts, nails and rebar provide incomplete shear connection and lead to partial composite interaction

In the present slip model, slip modulus K_s is employed to model the partial interaction effects at the interlayers and only linear part of the load-slip curve is considered. Hence, the relation between the interlayer slip displacement and slip load is determined through the constitutive laws as below,

$$V_s = K_s \cdot u_s \tag{2-4}$$

in which V_s is slip load per unit length, K_s is the constant slip modulus and u_s is corresponding interlayer slip displacement.

In the case of infinite slip modulus ($K_s = \infty$), shear connection exhibits perfect composite interactions and zero slip modulus ($K_s = 0$) indicates no composite interactions. Each case indicates upper and lower bounds for the composite action of the multi-layered structure.

Chapter 3. Beam Finite Element with Slip Mode

3.1 Continuum Mechanics based Beam Formulation

Continuum mechanics based beam formulations have been widely used for the analysis of general beam structures. Since the beam formulations are based on 3-D continuum mechanics, general 3-D curved and twisted geometries including fully coupled complete strains can be easily represented. In addition, the formulation form is straightforward. In spite of these advantages, the original degenerated continuum beam elements can be applied to only rectangular cross-sections in general. Recently, Yoon et al. [4] developed the concept of continuum mechanics based beam elements degenerated from assemblages of 3-D solid elements, which can model the arbitrary beam cross-sections. The beam formulation proposed by Yoon et al. is introduced briefly as follows.

3.1.1 Interpolation of Geometry

The geometry interpolation of the solid element m represented by 3-D shape function $h_i(r,s,t)$ is defined in the Cartesian coordinate system as below,

$$ {}^{t}\mathbf{x}^{(m)} = \sum_{i=1}^{n} h_i(r,s,t)\, {}^{t}\mathbf{x}_i^{(m)} \tag{3-1}$$

in which ${}^{t}\mathbf{x}^{(m)}$ is the material position vector of solid element m, ${}^{t}\mathbf{x}_i^{(m)}$ are the position vector of node i, n is the total number of nodes in the beam and t is time parameter. If all the nodes of solid elements are located on the cross-sectional plane k as depicted in Figure3.1, the geometry interpolation of the solid element m can be expressed by 1-D shape function $h_k(r)$ and 2-D shape function $h_j(s,t)$ and the position vector of cross-sectional node,

$$ {}^{t}\mathbf{x}^{(m)} = \sum_{k=1}^{q} h_k(r) \sum_{j=1}^{p} h_j(s,t)\, {}^{t}\mathbf{x}_k^{j(m)} \tag{3-2}$$

where ${}^{t}\mathbf{x}_k^{j(m)}$ is the position vector of the j th cross-sectional node in solid element m positioned on the cross-sectional plane k, q is the number of the cross-sectional planes k and p is the number of nodes in solid element m.

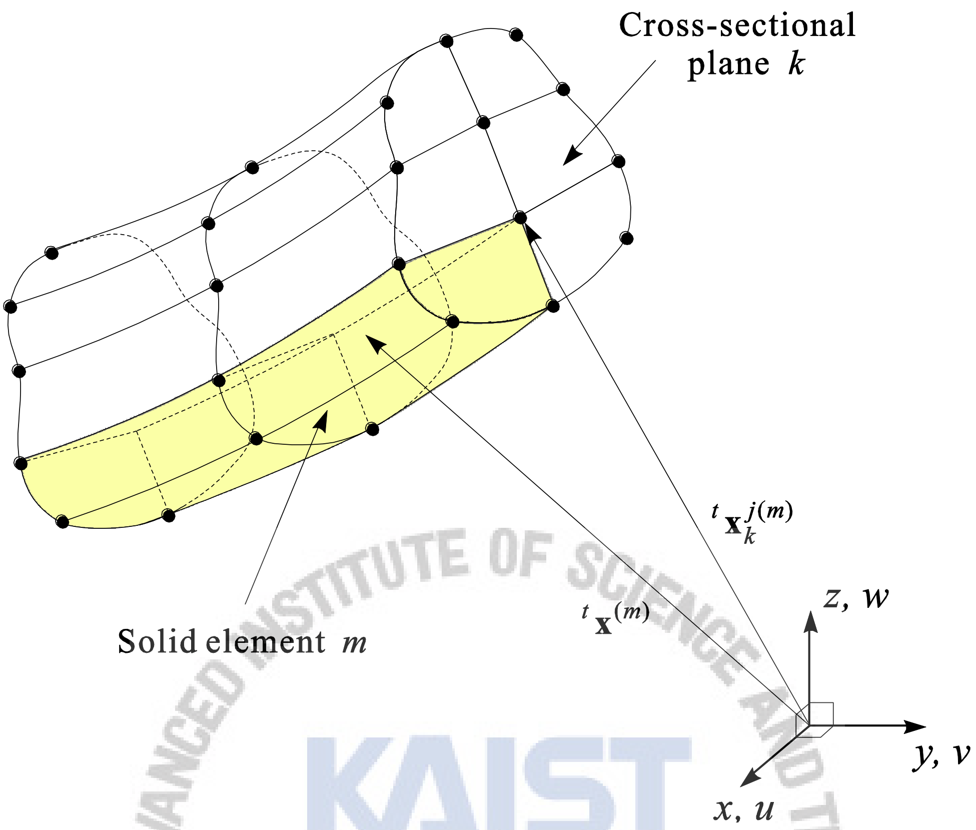

Figure3.1 An assemblage of 3D solid element that has arbitrary cross-section geometry

Under the assumption that plane cross-sections originally normal to the mid-line of the beam remain plane and undistorted during deformations but not necessarily normal to the mid-line of the deformed beam (Timoshenko 1970), a solid element behaves as a beam and therefore, solid element m can be substituted by sub-beam m. As a result, based on the assumption of Timoshenko beam theory, the position vector of j th cross-sectional node in sub-beam m $^{t}\mathbf{x}_{k}^{j(m)}$ can be represented by

$$^{t}\mathbf{x}_{k}^{j(m)} = {}^{t}\mathbf{x}_{k} + \bar{y}_{k}^{j(m)}\,{}^{t}\mathbf{V}_{\bar{y}}^{k} + \bar{z}_{k}^{j(m)}\,{}^{t}\mathbf{V}_{\bar{z}}^{k} \tag{3-3}$$

where $^{t}\mathbf{x}_{k}$ are the position vectors of beam node k placed at the origin C_k, $\bar{y}_{k}^{j(m)}$ and $\bar{z}_{k}^{j(m)}$ indicate the coordinate of the j th cross-sectional node in sub-beam m defined in cross-sectional Cartesian coordinate system. The cross-sectional Cartesian coordinate system is determined by $^{t}\mathbf{V}_{\bar{y}}^{k}$ and $^{t}\mathbf{V}_{\bar{z}}^{k}$, which are the unit director vectors at cross-sectional plane k and are normal to each other, see Figure 3.2.

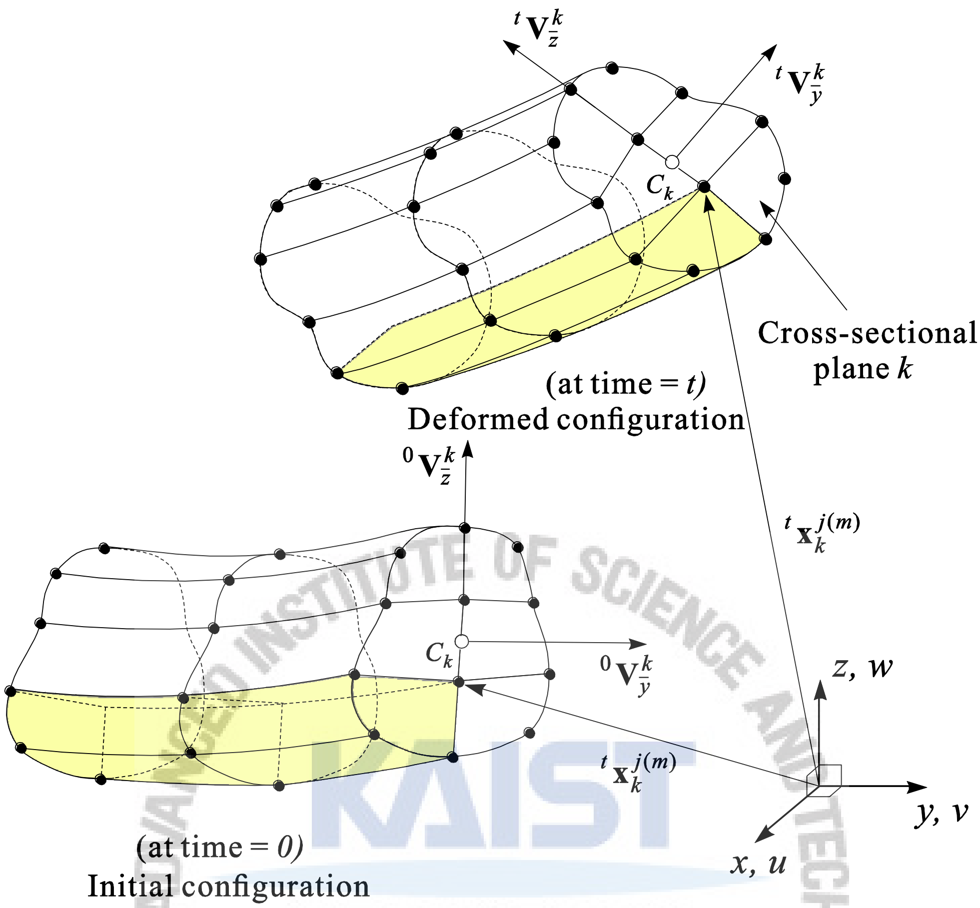

Figure 3.2 A 3-node continuum mechanics based beam element that has arbitrary cross-section geometry in the configuration at time t and at time 0

Consequently, the material position vector of sub-beam m at time t ${}^{t}\mathbf{x}^{(m)}$ can be obtained as follows.

$$ {}^{t}\mathbf{x}^{(m)} = \sum_{k=1}^{q} h_k(r)\,{}^{t}\mathbf{x}_k + \sum_{k=1}^{q} h_k(r)\bar{y}_k^{(m)}\,{}^{t}\mathbf{V}_{\bar{y}}^{k} + \sum_{k=1}^{q} h_k(r)\bar{z}_k^{(m)}\,{}^{t}\mathbf{V}_{\bar{z}}^{k} \tag{3-4} $$

$$ \text{with} \quad \bar{y}_k^{(m)} = \sum_{j=1}^{p} h_j(s,t)\bar{y}_k^{j(m)}, \quad \bar{z}_k^{(m)} = \sum_{j=1}^{p} h_j(s,t)\bar{z}_k^{j(m)} \tag{3-5} $$

Eq. (3-5) describes the material position of sub-beam m on the cross-sectional Cartesian coordinate system that interpolated by 2-D shape function and cross-sectional nodes of the sub-beam m. The material position vector of the beam is composed of the assemblage of the sub-beam m aligned in the longitudinal direction of the beam. The longitudinal reference line connecting the each beam node is used to define the geometry of the beam and the beam node at the origin C_k can be located on the cross-sectional plane k Therefore, the continuum mechanics based beam finite element is obtained by the beam nodes on the cross-sectional plane k and cross-sectional discretization at each beam node, see Figure 3.3.

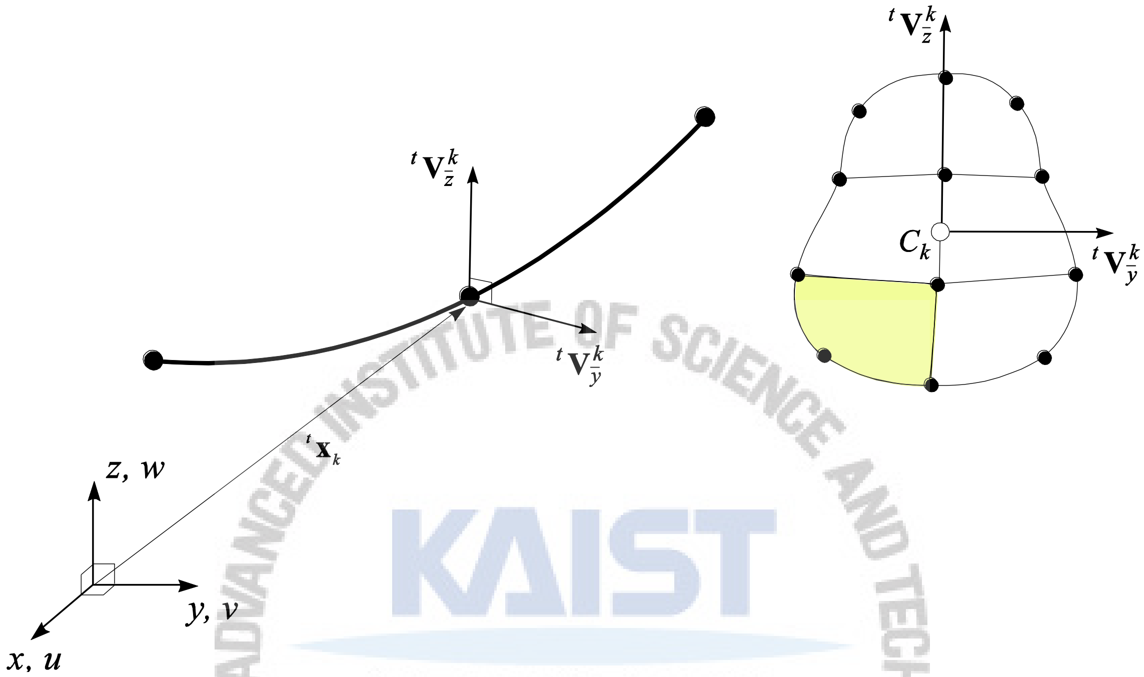

Figure 3.3 Cross-sectional discretization of continuum mechanics beam finite element. (a) 3-node beam finite element, (b) Cross-sectional discretization at beam node k

3.1.2 Interpolation of Displacement

The displacement interpolation of sub-beam m is derived through the interpolation of geometry as below (Bathe 1996),

$$\mathbf{u}^{(m)} = \sum_{k=1}^{q} h_k(r)\mathbf{u}_k + \sum_{k=1}^{q} h_k(r)\bar{y}_k^{(m)}({}^t\mathbf{V}_{\bar{y}}^k - {}^0\mathbf{V}_{\bar{y}}^k) + \sum_{k=1}^{q} h_k(r)\bar{z}_k^{(m)}({}^t\mathbf{V}_{\bar{z}}^k - {}^0\mathbf{V}_{\bar{z}}^k) \tag{3-6}$$

where $\mathbf{u}^k = \begin{bmatrix} u^k & v^k & w^k \end{bmatrix}^T$, ${}^t\mathbf{V}_{\bar{y}}^k$ and ${}^t\mathbf{V}_{\bar{z}}^k$ denote the director vectors of cross-sectional plane k in the configuration at time t. The displacement vector of sub-beam m is obtained by the nodal displacement vector at beam node, which is $\mathbf{u}_k$, and the material position of the sub-beam m on the cross-sectional plane k.

For the parametrization of finite rotations, Rodrigues formula is employed,

$$\mathbf{R}(\boldsymbol{\theta}^k) = \mathbf{I} + \frac{\sin\theta^k}{\theta^k}\hat{\mathbf{R}}(\boldsymbol{\theta}^k) + \frac{1-\cos\theta^k}{{\theta^k}^2}\hat{\mathbf{R}}(\boldsymbol{\theta}^k)^2 \tag{3-7}$$

$$\text{with } \boldsymbol{\theta}_k = \begin{bmatrix} \theta_x^k \\ \theta_y^k \\ \theta_z^k \end{bmatrix},\ \theta^k = \sqrt{{\theta_x^k}^2 + {\theta_y^k}^2 + {\theta_z^k}^2},\ \hat{\mathbf{R}}(\boldsymbol{\theta}^k) = \begin{bmatrix} 0 & -\theta_z^k & \theta_y^k \\ \theta_z^k & 0 & -\theta_x^k \\ -\theta_y^k & \theta_x^k & 0 \end{bmatrix} \tag{3-8}$$

where θ_x^k, θ_y^k and θ_z^k are the incremental Eulerian angles from time 0 to t, and $\hat{\mathbf{R}}(\boldsymbol{\theta}^k)$ is the skew-symmetric matrix operator. The Rodrigues formula can be written as polynomial function in terms of the incremental Eulerian angle vector $\boldsymbol{\theta}_k$ by applying Taylor expansion.

$$\mathbf{R}(\boldsymbol{\theta}^k) = \mathbf{I} + \hat{\mathbf{R}}(\boldsymbol{\theta}^k) + \frac{1}{2!}\hat{\mathbf{R}}(\boldsymbol{\theta}^k)^2 + \frac{1}{3!}\hat{\mathbf{R}}(\boldsymbol{\theta}^k)^3 + \frac{1}{4!}\hat{\mathbf{R}}(\boldsymbol{\theta}^k)^4 + \cdots \tag{3-9}$$

Then, the director vectors at time t can be expressed as

$${}^t\mathbf{V}_{\bar{x}}^k = \mathbf{R}(\boldsymbol{\theta}^k)\,{}^0\mathbf{V}_{\bar{x}}^k,\quad {}^t\mathbf{V}_{\bar{y}}^k = \mathbf{R}(\boldsymbol{\theta}^k)\,{}^0\mathbf{V}_{\bar{y}}^k \text{ and } {}^t\mathbf{V}_{\bar{z}}^k = \mathbf{R}(\boldsymbol{\theta}^k)\,{}^0\mathbf{V}_{\bar{z}}^k . \tag{3-10}$$

Accordingly, the displacement interpolation of sub-beam m is obtained as below.

$$\mathbf{u}^{(m)} = \sum_{k=1}^{q} h_k(r)\mathbf{u}_k + \sum_{k=1}^{q} h_k(r)\bar{y}_k^{(m)}(\mathbf{R}(\boldsymbol{\theta}^k) - \mathbf{I})\,{}^0\mathbf{V}_{\bar{y}}^k + \sum_{k=1}^{q} h_k(r)\bar{z}_k^{(m)}(\mathbf{R}(\boldsymbol{\theta}^k) - \mathbf{I})\,{}^0\mathbf{V}_{\bar{z}}^k \tag{3-11}$$

As a consequence of the first order approximation of the Rodrigues formula, Eq.(3-10) becomes

$$\mathbf{u}^{(m)} = \sum_{k=1}^{q} h_k(r)\mathbf{u}_k + \sum_{k=1}^{q} h_k(r)\bar{y}_k^{(m)}\hat{\mathbf{R}}(\theta^k)\,{}^0\mathbf{V}_{\bar{y}}^k + \sum_{k=1}^{q} h_k(r)\bar{z}_k^{(m)}\hat{\mathbf{R}}(\theta^k)\,{}^0\mathbf{V}_{\bar{z}}^k . \tag{3-12}$$

In Eq.(3-11), the displacement field of the whole beam composed of the sub-beam m is determined by the nodal displacement vector at each beam node which has three translations and three rotations, see Eq.(3-12).

$$\mathbf{U}_k = \begin{bmatrix} u_k & v_k & w_k & \theta_x^k & \theta_y^k & \theta_z^k \end{bmatrix}^T \tag{3-13}$$

Therefore, the behavior of the beam can be modeled by a single beam element having cross-sectional discretization at each cross-section k.

The displacement field in Eq. (3-12) can be extended to generalized displacement field by adding other displacement modes as below,

$$\mathbf{u}_g^{(m)} = \mathbf{u}^{(m)} + \mathbf{u}_a^{(m)} \tag{3-14}$$

in which $\mathbf{u}_g^{(m)}$ is the generalized displacement field and $\mathbf{u}_a^{(m)}$ is the additional displacement mode such as warping displacements and displacements for cross-sectional distortions. In the present research, the slip modes is added to the basic displacement field, for the analysis of the multi-layered composite beam with interlayer slips. The beam formulation including additional slip modes is explained in next section.

3.2 Enriched Beam Formulation with the Slip Mode

In order to consider interlayer slips in the beam due to the partial interaction effect, enriched displacement field with the additional displacement field, which is slip mode for slip displacements and corresponding slip DOFs are employed,

$$\mathbf{u}_g^{(m)} = \mathbf{u}^{(m)} + \mathbf{u}_s^{(m)} \tag{3-15}$$

where $\mathbf{u}_s^{(m)}$ represents the slip modes.

3.2.1 Interpolation of Displacement including Interlayer Slips

The geometry interpolation of the beam including slip displacements that corresponds to sub-beam m at time t is obtained as below,

$${}^t\mathbf{x}^{(m)} = \sum_{k=1}^{q} h_k(r)\,{}^t\mathbf{x}_k + \sum_{k=1}^{q} h_k(r)\bar{y}_k^{(m)}\,{}^t\mathbf{V}_{\bar{y}}^k + \sum_{k=1}^{q} h_k(r)\bar{z}_k^{(m)}\,{}^t\mathbf{V}_{\bar{z}}^k + \sum_{k=1}^{q} h_k(r)\sum_{i=1}^{l} f_k^{i(m)}(s,t)\,{}^t\alpha_k^i\,{}^t\mathbf{V}_{\bar{x}}^k \tag{3-16}$$

in which ${}^t\mathbf{V}_{\bar{x}}^k$ is the director vector normal to cross-sectional plane k defined by ${}^t\mathbf{V}_{\bar{x}}^k = {}^t\mathbf{V}_{\bar{y}}^k \times {}^t\mathbf{V}_{\bar{z}}^k$, $f_k^{i(m)}(s,t)$ is the slip function at beam node k, α_k^i is the corresponding slip degree of freedom at beam node k and l denotes the number of slip degree of freedoms. Consequently, the displacement interpolation of sub-beam m including slip modes is derived from the interpolation of geometry.

$$\mathbf{u}^{(m)} = {}^t\mathbf{x}^{(m)} - {}^0\mathbf{x}^{(m)} = \sum_{k=1}^{q} h_k(r)\mathbf{u}_k + \sum_{k=1}^{q} h_k(r)\bar{y}_k^{(m)}\hat{\mathbf{R}}(\boldsymbol{\theta}^k)\,{}^t\mathbf{V}_{\bar{y}}^k + \sum_{k=1}^{q} h_k(r)\bar{z}_k^{(m)}\hat{\mathbf{R}}(\boldsymbol{\theta}^k)\,{}^t\mathbf{V}_{\bar{z}}^k$$

$$+\sum_{k=1}^{q} h_k(r)\sum_{i=1}^{l} f_k^{i(m)}(s,t)[\alpha_k^i\mathbf{I} + {}^0\alpha_k^i\hat{\mathbf{R}}(\boldsymbol{\theta}^k)]\,{}^t\mathbf{V}_{\bar{x}}^k \tag{3-17}$$

In Eq. (3-17), the displacement field is represented by $(6+l)$ DOFs at each beam node k that has (three translations, three rotations and slip DOFs

$$\mathbf{U}_k = \begin{bmatrix} u_k & v_k & w_k & \theta_x^k & \theta_y^k & \theta_z^k & \boldsymbol{\alpha}_k^{\mathrm{T}} \end{bmatrix}^T, \tag{3-18}$$

in which $\boldsymbol{\alpha}_k = \begin{bmatrix} \alpha_k^1 & \alpha_k^2 & \dots & \alpha_k^n \end{bmatrix}^T$ and n is the number of interlayers. Normally, two slip modes that are composed of bending slip mode and axial slip mode are required for two-dimensional analysis and it can be easily extended to three-dimensional analysis with another bending slip mode corresponding to the extended dimension.

3.2.2 Calculation Procedure of Slip Function

Slip modes are modeled by slip functions with slip DOFs in the beam formulation. The slip modes are composed of bending slip mode and axial slip mode and each slip mode can be represented by corresponding bending slip functions $f_k^b(s,t)$ and axial slip function $f_k^a(s,t)$ with bending slip DOF α_k^b and axial slip DOF α_k^a individually. The slip function is the step function defined over the cross-sectional plane k of a beam in which the value of the slip functions indicates the extent of deformation in ${}^t\mathbf{V}_{\bar{x}}^k$ direction.

3.2.2.1 Bending Slip Function

In the case of bending slip mode, the interlayer slip displacements s_i^b are derived as explained in section 2.2.1, see Eq.(2-2).

$$s_i^b = u_{i+1} - u_i + d_i\frac{\partial v}{\partial x} = d_i\theta\,,\quad i = 1,2,\cdots,n-1$$

Since each sub-beam has the same rotation according to the aforementioned assumptions, the interlayer slip displacements in bending mode s_i^b are proportional to d_i, which is the length between the centroid of sub-beam $i+1$ and the centroid of sub-beam i.

In the enriched beam formulation, the interlayer slips in the bending mode are modeled by the superposition of the behavior of a single beam and bending slip function $f_k^b(s,t)$ with bending slip DOF α_k^b. Because the single beam represents the average behavior of the association of the sub-beams, the cross-sectional plane k of the beam is located on the mean position between the interlayer slips. Consequently, the value of the bending slip function x_i^b indicates the extent of deformation in ${}^t\mathbf{V}_{\bar{x}}^k$ direction from the cross-sectional plane k of a beam as shown in Figure 3.4.

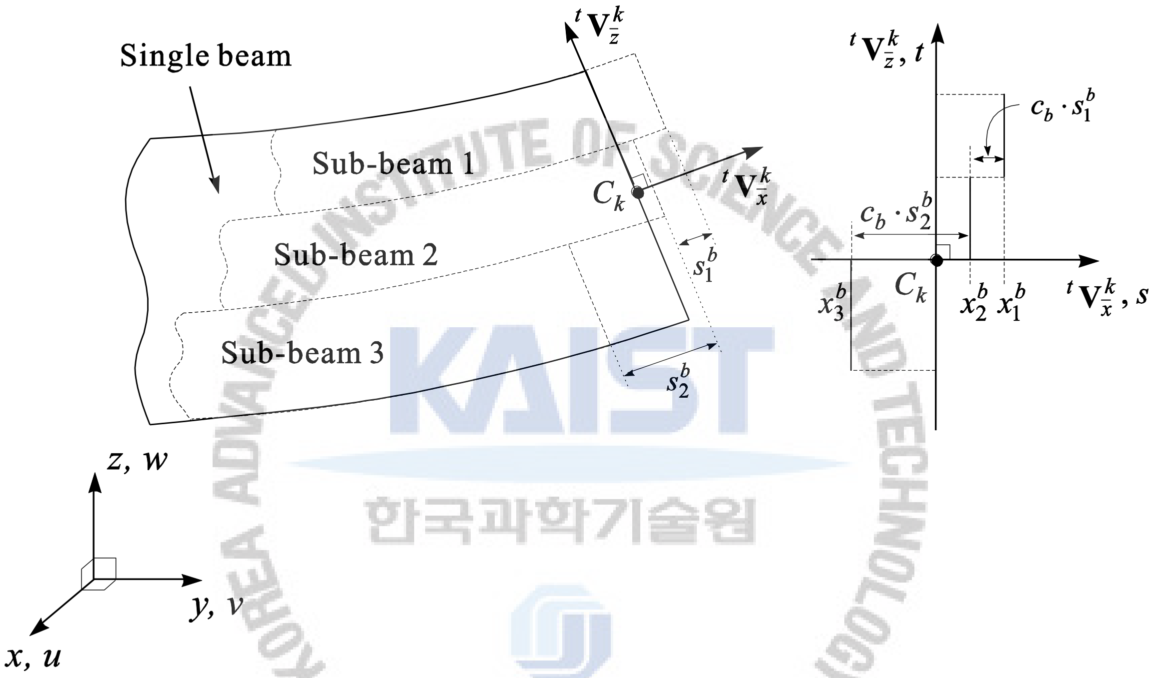

Figure 3.4 Bending slip function in three-layer beam model

In the bending slip function, the jumps at the discontinuity point indicates the extent of the interlayer slip displacements in the bending mode, which is proportional to the interlayer slips. The sum of the slip function value should be zero, since the cross-sectional plane k is located on the mean position between the interlayer slips. Therefore, the value of the bending slip function can be obtained through the equations as follows,

$$x_i^b - x_{i+1}^b = c_b \cdot s_i^b = c_b \cdot d_i\theta, \quad i = 1,2,\cdots,n-1 \tag{3-19}$$

$$\sum_{i=1}^{n} x_i^b = 0 \tag{3-20}$$

where c_b denotes constant coefficient in bending slip function.

Then, x_i^b is represented in terms of d_i

$$\mathbf{x}^b = \mathbf{\Psi}_b^{-1}\mathbf{r}_b \tag{3-21}$$

with $\mathbf{x}^b = \begin{bmatrix} x_1^b & x_2^b & \cdots & x_n^b \end{bmatrix}^{\mathrm{T}}$, $\mathbf{r}_b = \begin{bmatrix} d_1^b & d_2^b & \cdots & d_{n-1}^b & 0 \end{bmatrix}^{\mathrm{T}}$, $\mathbf{\Psi}_b = \begin{bmatrix} \mathbf{Q} \\ \mathbf{J}_{1,n} \end{bmatrix}$

and $\mathbf{Q} = [\mathbf{I}_n \quad \mathbf{0}] + [\mathbf{0} \quad -\mathbf{I}_n]$, where $\mathbf{I}_n$ is $n \times n$ identity matrix and $\mathbf{J}_{1,n}$ is $1 \times n$ matrix of ones.

3.2.2.2 Axial Slip Function

In the case of axial slip mode, the interlayer slip displacements s_i^a are derived as explained in section 2.2.2, see Eq.(2-3).

$$s_i^a = u_{i+1} - u_i = \frac{P_{i+1}L}{E_{i+1}A_{i+1}} - \frac{P_i L}{E_i A_i} = \frac{P_0 L}{A_0}\left(\frac{1}{E_{i+1}} - \frac{1}{E_i}\right), \quad i = 1, 2, \cdots, n-1$$

Since each sub-beam is subjected to uniform axial stress P_0/A_0 due to the aforementioned assumptions, the interlayer slip displacements in axial mode s_i^a are proportional to $\left(1/E_{i+1} - 1/E_i\right)$.

Similar to the preceding section, the interlayer slips in the axial mode are modeled by the superposition of the behavior of a single beam and axial slip function $f_k^a(s,t)$ with axial slip DOF α_k^a and the cross-sectional plane k of the beam is located on the mean position between the interlayer slips. Therefore, the value of the axial slip function x_i^a indicates the extent of deformation in ${}^t\mathbf{V}_{\bar{x}}^k$ direction from the cross-sectional plane k of a beam as shown in Figure 3.5.

The jumps at the discontinuity point of the axial slip function indicates the extent of the interlayer slip displacements in the axial mode, which is proportional to the interlayer slips and the sum of the axial slip function value should be zero, since the cross-sectional plane k is located on the mean position between the interlayer slips . As a result, the value of the axial slip function can be obtained through the equations as follows,

$$x_i^a - x_{i+1}^a = c_a \cdot s_i^a = c_a \cdot \left(\frac{1}{E_i} - \frac{1}{E_{i+1}} \right), \quad i = 1,2,\cdots,n-1 \tag{3-22}$$

$$\sum_{i=1}^{n} x_i^a = 0 \tag{3-23}$$

where c_a denotes constant coefficient in axial slip function.

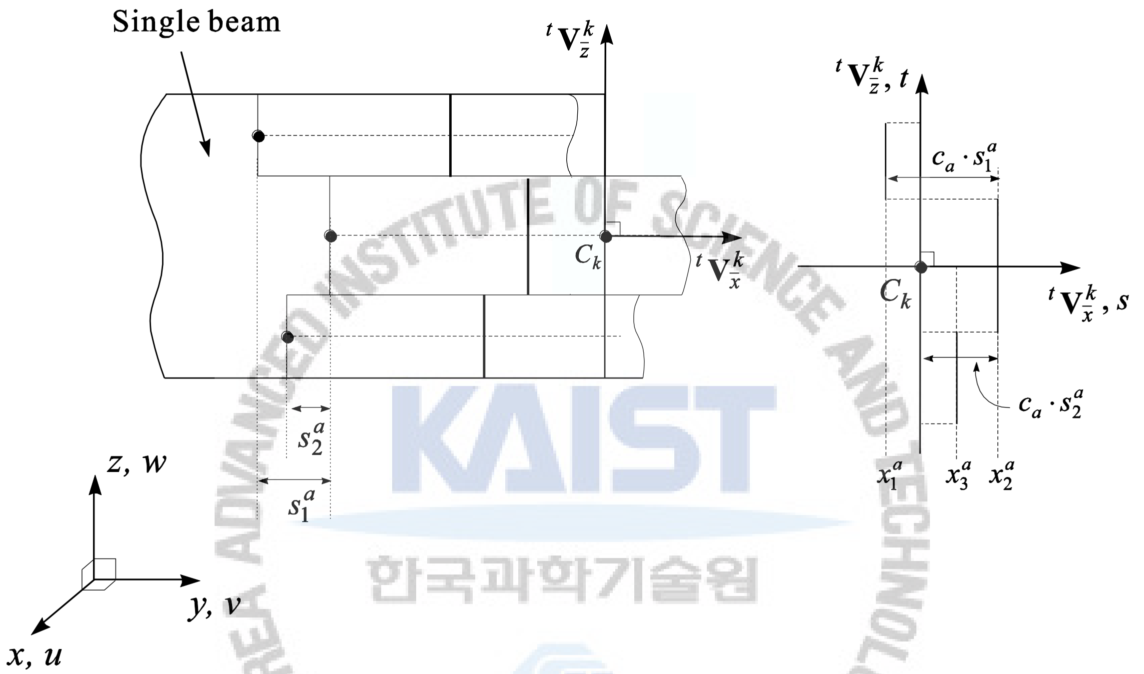

Figure 3.5 Axial slip function in the three-layer beam model

Then, x_i^a is represented in terms of E_i

$$\mathbf{x}^a = \mathbf{\Psi}_a^{-1} \mathbf{r}_a \tag{3-24}$$

with $\mathbf{x}^a = \begin{bmatrix} x_1^a & x_2^a & \cdots & x_n^a \end{bmatrix}^{\mathrm{T}}$, $\mathbf{r}_b = \begin{bmatrix} 1/E_1 - 1/E_2 & 1/E_2 - 1/E_3 & \cdots & 1/E_{n-1} - 1/E_n & 0 \end{bmatrix}^{\mathrm{T}}$, $\mathbf{\Psi}_a = \begin{bmatrix} \mathbf{Q} \\ \mathbf{J}_{1,n} \end{bmatrix}$

and $\mathbf{Q} = [\mathbf{I}_n \quad \mathbf{0}] + [\mathbf{0} \quad -\mathbf{I}_n]$, where $\mathbf{I}_n$ is $n \times n$ identity matrix and $\mathbf{J}_{1,n}$ is $1 \times n$ matrix of ones.

Note that both slip function is not unique, however their value should satisfies the specific ratio corresponding to the slip mode.

Chapter 4. Finite Element Analysis Procedure

4.1 The Variational Formulation of the Beam with Interlayer Slips

The solution of the displacement-based finite element analysis is based on the variational method. The governing equations of system can be constructed with relative ease by employing the variational method, since scalar quantities are considered rather than vector quantities in the variational formulation. In the present research, the variational formulation of the beam model including the partial interaction effect with interlayer slips was derived from the principle of virtual work for the finite element analysis. The concept of the general principle of virtual work is introduced briefly as follows.

4.1.1 The Principle of Virtual Work

The principle of virtual work states that the total external virtual work done by the external loads under the compatible displacements imposed on the body in its state of equilibrium is equal to the total internal virtual work done by internal force as described in Eq.(4-1).

$$\int_{{}^0V} \delta\boldsymbol{\varepsilon}^T \boldsymbol{\tau} dV = \int_{{}^0V} \delta\mathbf{u}^T \mathbf{f}^B dV + \int_{S_f} \delta\mathbf{u}^T \mathbf{f}^S dS \qquad (4\text{-}1).$$

in which $\mathbf{f}^B$ are externally applied body forces in the volume (force per unit volume) and $\mathbf{f}^S$ are surface tractions on the surface S_f (force per unit surface area), $\delta\mathbf{u}$ are the virtual displacements, $\delta\boldsymbol{\varepsilon}$ are the corresponding virtual strains, $\boldsymbol{\tau}$ are stresses corresponding to $\boldsymbol{\varepsilon}$, ${}^0V$ and ${}^tV$ are volume in the initial configuration at time 0, in the current configuration at time t respectively, and initial stresses are assumed to be zeros, see Figure 4.1. The body is subjected to surface tractions $\mathbf{f}^S$ on the surface area S_f and is supported on the area S_u with corresponding prescribed displacements $\mathbf{U}^{S_u}$. Assuming that all displacements on S_u are prescribed, $S_u \cup S_f = S$ and $S_u \cap S_f = 0$.

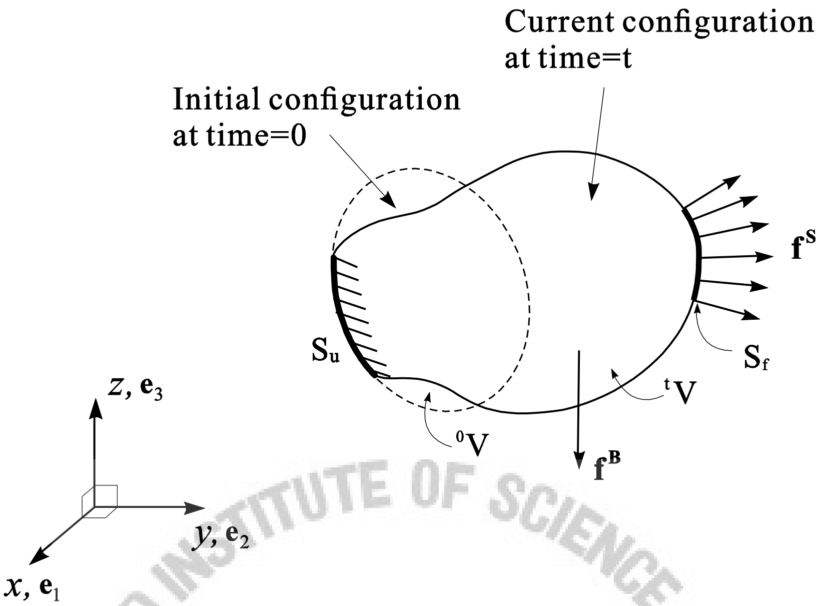

Figure 4.1 A body in its equilibrium state subjected to body force and surface tractions.

The virtual displacements $\delta\mathbf{u}$ must be a continuous virtual displacement field and satisfies prescribed displacements on S_u. The virtual strain $\delta\boldsymbol{\varepsilon}$ are calculated by the differentiations from the assumed virtual displacements $\delta\mathbf{u}$. Note that all integrations are carried out over the initial configuration of the body that unaffected by the imposed virtual displacements.

4.1.2 The Weak Form of the Beam Formulation

Unlike conventional beam that has no flexible interlayers between the components, partial interactions are caused due to the partial transfer of shear stresses at the interlayers in the multi-layered composite beam with deformable shear connections. Consequently, the partial interaction effect and resulting interlayer slips should be considered in the governing equations.

In the present beam model, the constant slip modulus K_s is employed to model the partial interaction effect between the layers and only linear part of the load-slip curve is considered. Therefore, The constitutive law that represents the relation between the interlayer slip displacement and slip load is used as below.

$$V_s = K_s \cdot u_s$$

Also, assuming zero initial stresses, the stresses $\boldsymbol{\tau}$ can be represented by

$$\boldsymbol{\tau} = \mathbf{C}\boldsymbol{\varepsilon}, \tag{4-2}$$

where $\mathbf{C}$ is the stress-strain matrix of the material. Accordingly, the weak form of the present beam formulation can be obtained by employing the Eq. (4-2) in the principle of virtual work as expressed in Eq. (4-2).

$$\int_{V_0} \delta\boldsymbol{\varepsilon}^T \mathbf{C}\boldsymbol{\varepsilon} \mathrm{d}V + \int_L \delta\mathbf{u}_s{}^T \mathbf{K}_s \mathbf{u}_s \mathrm{d}L = \int_{V_0} \delta\mathbf{u}^T \mathbf{f}^B \mathrm{d}V + \int_{S_f} \delta\mathbf{u}^T \mathbf{f}^S \mathrm{d}S \tag{4-3}$$

where $\mathbf{u}_s$ is interlayer slip displacement vector and $\mathbf{K}_s$ is slip modulus matrix,

$$\mathbf{u}_s = \begin{bmatrix} u_{s1} & u_{s2} & \cdots & u_{s(i-1)} \end{bmatrix}^{\mathrm{T}}, \quad i = 1,2\ldots n \tag{4-4}$$

$$\mathbf{K}_s = \begin{bmatrix} \mathrm{K}_{s1} & 0 & 0 & 0 \\ 0 & \mathrm{K}_{s2} & 0 & 0 \\ \vdots & \vdots & \ddots & \vdots \\ 0 & 0 & 0 & \mathrm{K}_{si} \end{bmatrix}, \quad i = 1,2\ldots n \tag{4-5}$$

with the number of layers n.

4.2 Finite Element Discretization

For finite element analysis, finite element formulations are derived based on linearized covariant Green-Lagrange strain. Then, the multi-layered composite beam is discretized by two-node beam element with slip modes and the standard numerical integration procedure is used.

4.2.1 Green-Lagrange Strain

The Green-Lagrange strain tensor for the sub-beam defined with respect to the initial coordinates can be written in terms of the Cauchy-Green deformation tensor as below,

$${}_0^t\boldsymbol{\varepsilon}^{(m)} = \frac{1}{2}({}_0^t\mathbf{X}^{(m)\mathrm{T}}\,{}_0^t\mathbf{X}^{(m)} - \mathbf{I}) = \frac{1}{2}({}_0^t\mathbf{C}^{(m)} - \mathbf{I}) \quad \text{with} \quad {}_0^t\mathbf{X}^{(m)} = \frac{\partial^t x_i^{(m)}}{\partial^0 x_j^{(m)}}, \tag{4-6}$$

in which ${}_0^t\mathbf{X}^{(m)}$ is deformation gradient for sub-beam m.

In global Cartesian coordinate system, the components of the Green-Lagrange strain tensor ${}_0^t\boldsymbol{\varepsilon}^{(m)}$ is represented by

$$
{}_0^t\varepsilon_{ij}^{(m)} = \frac{1}{2}\left(\frac{\partial^t u_i}{\partial^0 x_j} + \frac{\partial^t u_j}{\partial^0 x_i} + \frac{\partial^t u_k}{\partial^0 x_i}\frac{\partial^t u_k}{\partial^0 x_j} \right) \tag{4-7}
$$

Also, the Green-Lagrange strain tensor can be written in terms of the covariant components in general coordinate as follows,

$$
{}_0^t\tilde{\varepsilon}_{ij}^{(m)} = \frac{1}{2}({}^t\mathbf{g}_i^{(m)} \cdot {}^t\mathbf{g}_j^{(m)} - {}^0\mathbf{g}_i^{(m)} \cdot {}^0\mathbf{g}_j^{(m)}) \quad \text{with} \quad {}^t\mathbf{g}_i^{(m)} = \frac{\partial^t\mathbf{x}^{(m)}}{\partial r_i} \tag{4-8}
$$

where ${}^t\mathbf{g}_i^{(m)}$ is natural base vectors for sub-beam m. Note that in Eq. (4-7) and Eq. (4-8) the strain components are considered up to quadratic order. In local Cartesian coordinate system, the local Green-Lagrange strain tensor ${}_0^t\bar{\varepsilon}_{ij}^{(m)}$ is obtained through the transformation of the basis vectors, see Figure 4.2.

$$
(\mathbf{t}_i \otimes \mathbf{t}_j){}_0^t\bar{\varepsilon}_{ij}^{(m)} = ({}^0\mathbf{g}^{k(m)} \otimes {}^0\mathbf{g}^{l(m)}){}_0^t\tilde{\varepsilon}_{kl}^{(m)} \tag{4-9}
$$

In Eq. (4-9), ${}^0\mathbf{g}^{i(m)}$ denote the contravariant base vectors defined by

$$
{}^0\mathbf{g}^{i(m)} \cdot {}^0\mathbf{g}_j^{(m)} = \delta_j^i,
$$

in which δ_j^i is the Kronecker delta.

The covariant Green-Lagrange strain can be decomposed as follows,

$$
{}_0^t\tilde{\varepsilon}_{ij}^{(m)} \approx {}_0^t\tilde{e}_{ij}^{(m)} + {}_0^t\tilde{\eta}_{ij}^{(m)} \tag{4-10}
$$

$$
\text{with} \quad {}_0^t\tilde{e}_{ij}^{(m)} = \frac{1}{2}({}^t\mathbf{g}_i^{(m)} \cdot \frac{\partial \mathbf{u}^{(m)}}{\partial r_j} + {}^t\mathbf{g}_j^{(m)} \cdot \frac{\partial \mathbf{u}^{(m)}}{\partial r_i}) \quad \text{and} \quad {}_0^t\tilde{\eta}_{ij}^{(m)} = \frac{1}{2}\frac{\partial \mathbf{u}^{(m)}}{\partial r_i} \cdot \frac{\partial \mathbf{u}^{(m)}}{\partial r_j}. \tag{4-11}
$$

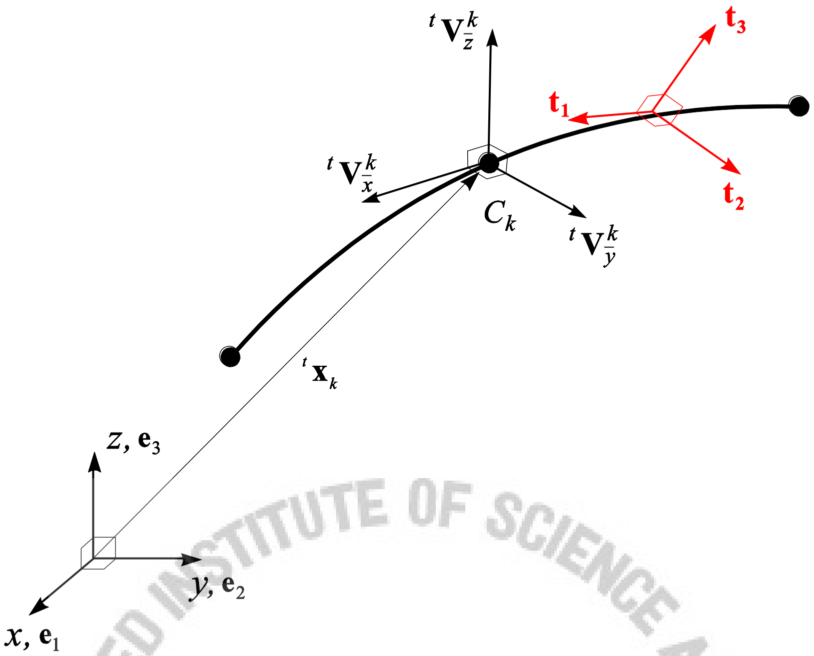

Figure 4.2 Global Cartesian coordinate system, cross-sectional coordinate system and local coordinate system in 3-node beam element

In the present research, finite element formulations is derived based on the linearized covariant Green-Lagrange strain of the sub-beam m ${}_0^t\tilde{e}_{ij}^{(m)}$ with the assumption of small deformation theory and five strain components (${}_0^t\tilde{e}_{11}^{(m)}$, ${}_0^t\tilde{e}_{12}^{(m)}$, ${}_0^t\tilde{e}_{21}^{(m)}$, ${}_0^t\tilde{e}_{13}^{(m)}$, ${}_0^t\tilde{e}_{31}^{(m)}$) are considered.

4.2.2 Finite Element Formulations

The displacement field of sub-beam m $\mathbf{u}^{(m)}$ was derived in the preceding chapter and the $\mathbf{u}^{(m)}$ was represented by $\mathbf{U}_k$, which is composed of $(6+l)$ number of global displacement components at all nodal points. Accordingly, the total nodal displacements vector is obtained as below in the q-node beam.

$$\mathbf{U} = \begin{bmatrix} \mathbf{U}_1^T & \mathbf{U}_2^T & \ldots\ldots & \mathbf{U}_q^T \end{bmatrix}^T \tag{4-12}$$

Then, the $\mathbf{u}^{(m)}$ can be represented in terms of $\mathbf{U}$ through the $\mathbf{H}^{(m)}$ matrix

$$\mathbf{u}^{(m)} = \mathbf{H}^{(m)}\mathbf{U}\,, \tag{4-13}$$

where $\mathbf{H}^{(m)}$ is so-called displacement interpolation matrix in the sub-beam m. Similarly, variation of the $\mathbf{u}^{(m)}$ is obtained as follows.

$$\delta\mathbf{u}^{(m)} = \mathbf{H}^{(m)}\delta\mathbf{U} \tag{4-14}$$

Also, linearized covariant components of the Green-Lagrange strain in the sub-beam m ${}_{0}^{t}\tilde{e}_{ij}^{(m)}$ and their variation can be written in terms of $\mathbf{U}$ and $\delta\mathbf{U}$ respectively as below,

$$\mathbf{e}^{(m)} = \mathbf{B}^{(m)}\mathbf{U} \tag{4-15}$$

$$\delta\mathbf{e}^{(m)} = \mathbf{B}^{(m)}\delta\mathbf{U}\,, \tag{4-16}$$

in which $\mathbf{B}^{(m)}$ is strain-displacement matrix. The rows of $\mathbf{B}^{(m)}$ are obtained by differentiating and combining rows of the matrix $\mathbf{H}^{(m)}$. Lastly, slip displacement and virtual slip displacement can be also obtained with respect to $\mathbf{U}$ and $\delta\mathbf{U}$.

$$\mathbf{u}_s^{(m)} = \mathbf{H}_s^{(m)}\mathbf{U} \tag{4-17}$$

$$\delta\mathbf{u}_s^{(m)} = \mathbf{H}_s^{(m)}\delta\mathbf{U} \tag{4-18}$$

Note that same interpolation is employed for real and virtual displacements.

The weak form of the beam formulation (Eq. 4-3) can be rewritten as a sum of integrations over the sub-beam m.

$$\sum_m \int_{V_0} \delta\mathbf{e}^{(m)T}\mathbf{C}^{(m)}\mathbf{e}^{(m)}\mathrm{d}V^{(m)} + \sum_m \int_L \delta\mathbf{u}_s^{(m)T}\mathbf{K}_s^{(m)}\mathbf{u}_s^{(m)T}\mathrm{d}L^{(m)}$$

$$= \sum_m \int_{V_0} \delta\mathbf{u}^{(m)T}\mathbf{f}^{(m)B}\mathrm{d}V^{(m)} + \sum_m \int_{S_f} \delta\mathbf{u}^{(m)T}\mathbf{f}^{S}\mathrm{d}S^{(m)} \tag{4-19}$$

Substituting the Eq. (4-13), Eq. (4-14), Eq. (4-15), Eq. (4-16), Eq. (4-17) and Eq. (4-18), the weak form is expressed in terms of the nodal displacement vector $\mathbf{U}$ and virtual nodal displacement vector $\delta\mathbf{U}$.

$$\delta \mathbf{U}^{\mathrm{T}}\left[\sum_m \int_{V_0} \mathbf{B}^{(m)T}\mathbf{C}^{(m)}\mathbf{B}^{(m)} \mathrm{d}V^{(m)} + \sum_m \int_L \mathbf{H}_s^{(m)T} \mathbf{K}_s^{(m)} \mathbf{H}_s^{(m)T} \mathrm{d}L^{(m)}\right]\mathbf{U}$$

$$= \delta \mathbf{U}^{\mathrm{T}}\left[\sum_m \int_{V_0} \mathbf{H}^{(m)T}\mathbf{f}^{(m)B} \mathrm{d}V^{(m)} + \sum_m \int_{S_f} \mathbf{H}^{(m)T}\mathbf{f}^{S} \mathrm{d}S^{(m)}\right] \tag{4-20}$$

As a result, linearized equilibrium equations is obtained as below

$$\mathbf{KU} = \mathbf{R} \tag{4-21}$$

where,

$$\mathbf{K} = \sum_{m=1}^{n} \int_{{}^0V^{(m)}} \mathbf{B}^{(m)^T}\mathbf{C}^{(m)}\mathbf{B}^{(m)} dV + \sum_{m=1}^{n} \int_{L^{(m)}} \mathbf{B}^{(m)^T}\mathbf{C}^{(m)}\mathbf{B}^{(m)} dV \tag{4-22}$$

$$\mathbf{R} = \sum_m \int_{V_0} \mathbf{H}^{(m)T}\mathbf{f}^{(m)B} \mathrm{d}V^{(m)} + \sum_m \int_{S_f} \mathbf{H}^{(m)T}\mathbf{f}^{S} \mathrm{d}S^{(m)} \tag{4-23}$$

4.2.3 Numerical Integration

To obtain stiffness matrix and load vector of the system, $2\times2\times2$ Gauss integration is employed for each sub-beam m. That is, there are two integration points in the longitudinal direction and 2×2 Gauss integration is carried out in the cross-sectional plane of sub-beam m ($s-t$ plane) as shown in Figure 4.3.

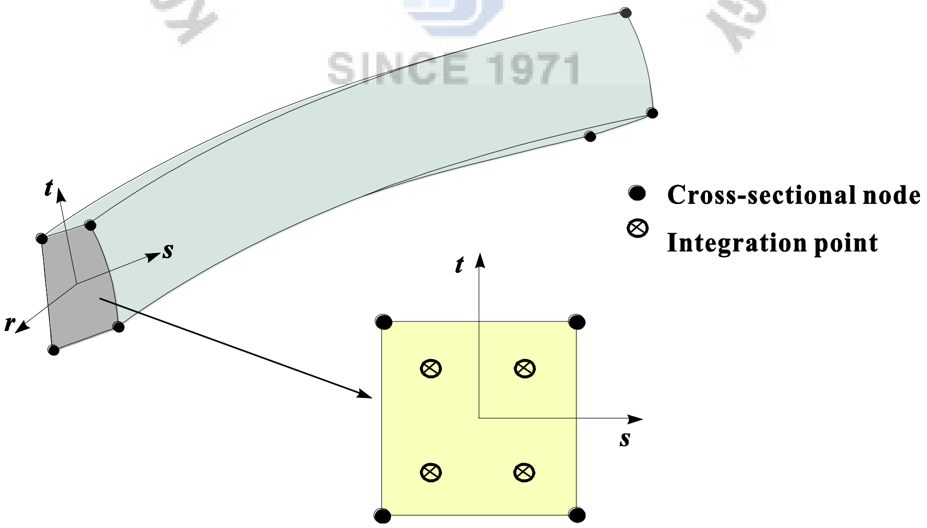

Figure 4.3 Gauss integration points in the sub-beam element m.

In the case of slender beam, the displacement-based isoparametric beam finite element becomes too stiff in bending, that is, the beam finite element locks. Therefore, MITC (Mixed Interpolation of Tensorial Components) scheme is used to remove shear lockings, Note that MITC scheme gives better performance compared to the reduced integration scheme especially for the complex beam geometry.

Chapter 5. Numerical Studies

5.1 Verification of the Proposed Model

The proposed beam finite element including interlayer slips is verified by comparing solutions with those found in literatures. In order to evaluate the partial interaction effects in the partially connected beam, the multi-layered composite beam with deformable connections is compared with the conventional beam that has perfect connections. Then, several numerical examples are presented to demonstrate accuracy and performance of the present model. The significant numerical results such as tip-displacements and mid-point displacements are compared to those obtained by other author.

5.1.1 Comparison with Conventional Beam

Two-layer and three-layer composite beam with deformable connections are compared to the case of corresponding perfectly connected beam, for different slip modulus to briefly assess the influence of the slip modulus between the layers on the partial interaction effect.

5.1.1.1 Two-layer Partially Connected Beam

Two-layer partially connected cantilever beam and perfectly connected cantilever beam, which is identical to the conventional beam with no interlayers are shown in Figure 5.1(a) and Figure 5.1(b).

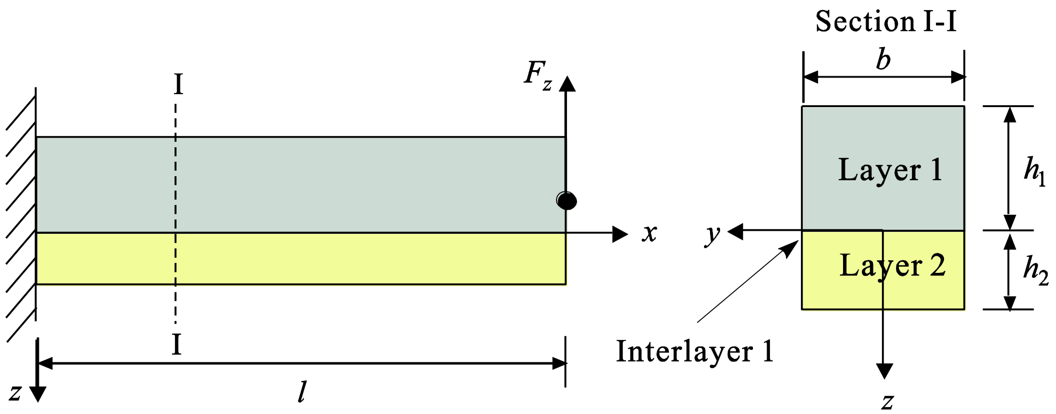

Figure 5.1(a) Two-layer partially connected beam subjected to tip vertical load F_z

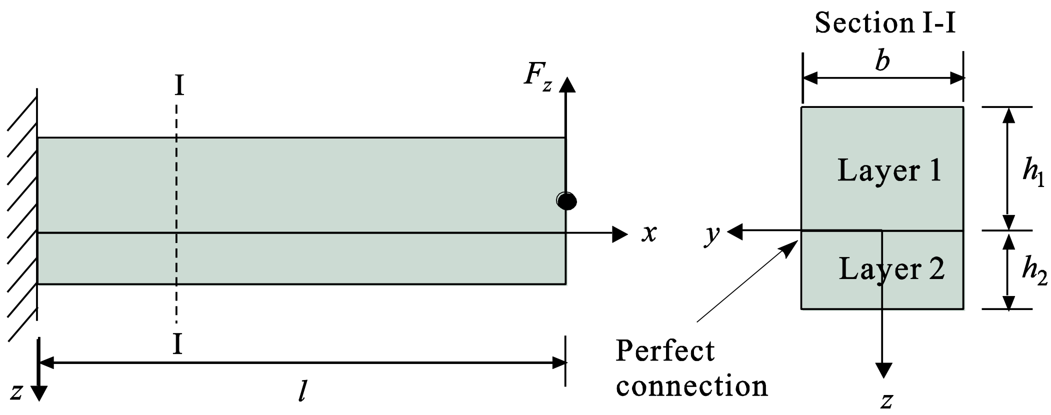

Figure 5.1(b) Two-layer perfectly connected beam subjected to tip vertical load F_z

Each layer of the beam has same Young's modulus, Poisson's ratio but different cross-section area. The beams are subjected to tip vertical load F_z. Geometry, loading condition and material properties are described in Table 5.1.

Geometry and Loading condition	Material property
$l = 100$ m	$E_1 = E_2 = 10^5$ N/m^2
$b = 1$m	$\upsilon_1 = \upsilon_2 = 0.5$
$h_1 = 2$m	
$h_2 = 1$m	
$F_z = 1N$	

Table 5.1 Geometry, material property loading condition and slip modulus for two-layer partially connected beam.

Both beams are modeled by five 2-node beam elements and the rectangular cross-section is discretized by 4-node cubic cross-sectional element. Deflections, deflection angles and interlayer slips at the tip of the partially connected beam are compared to those of the perfectly connected beam for increasing slip modulus value. It can be observed that the results of the two-layer partially connected beam converge to the solution of the conventional beam as slip modulus increases. It can be concluded that the present beam element gives reasonable solutions for modeling partial interaction effect. The results are depicted in Figure 5.2(a), Figure 5.2(b) and Figure 5.2(c).

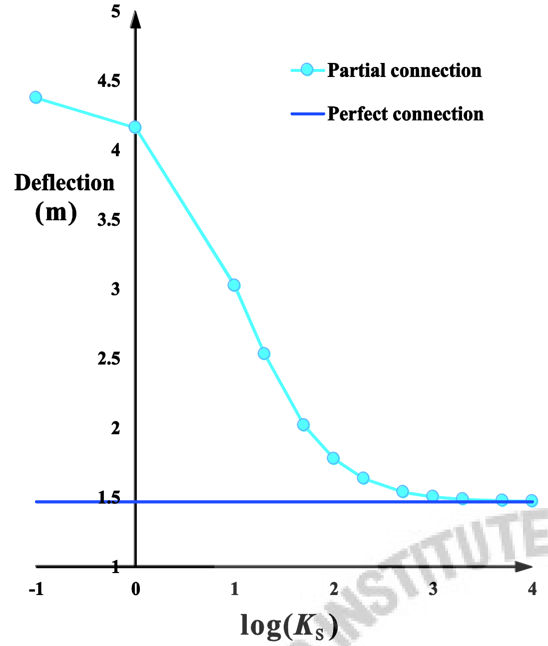

Figure 5-2(a) Deflections at the tip of the partially and perfectly connected beams

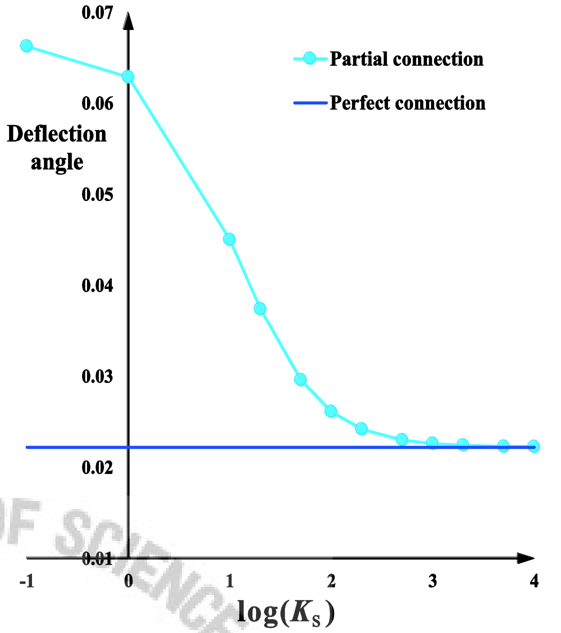

Figure 5-2(b) Deflection angles at the tip of the partially and perfectly connected beams

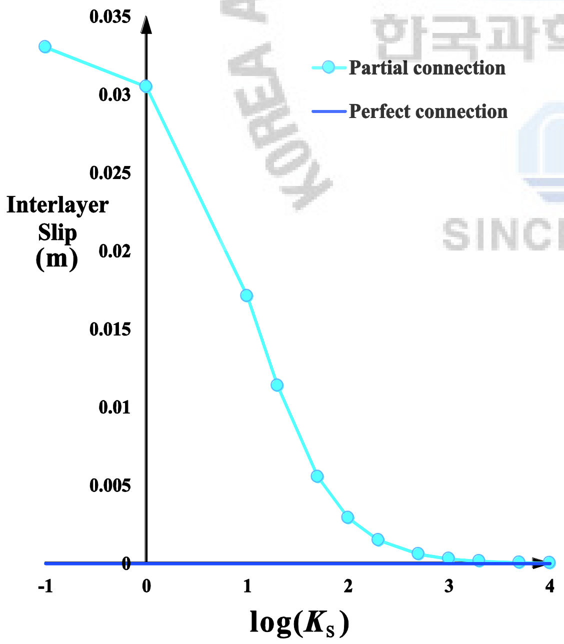

Figure 5-2(c) Interlayer slips at the tip of the partially and perfectly connected beams

5.1.1.2 Three-layer Composite Beam

Three-layer partially connected beam and perfectly connected beam identical to the conventional beam with no interlayers are shown in Figure 5.3(a) and Figure 5.3(b). Material properties, loading condition and geometry data are described in Table 5.2. Each beam is modeled by five 2-node beam elements and the rectangular cross-section is discretized by 4-node cubic cross-sectional element. Deflections, deflection angles and interlayer slips at the tip of the three-layer partially connected beam are compared to those of the conventional beam with no partial interaction effect, for increasing slip modulus value. Similar to preceding section, the results of the three-layer partially connected beam converge to the solution of the perfectly connected beam as slip modulus increases. The results are shown in Figure 5.4(a), Figure 5.4(b) and Figure 5.4(c).

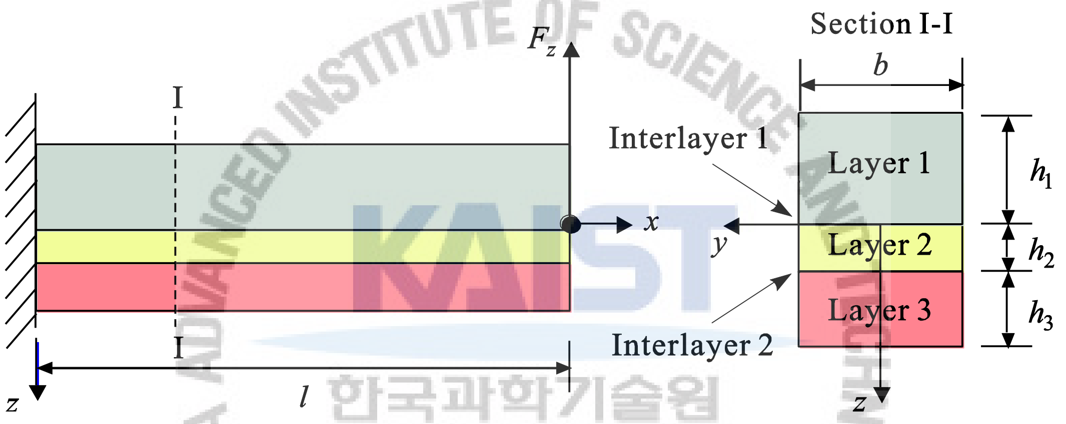

Figure 5.3(a) Three-layer partially connected beam subjected to tip vertical load F_z

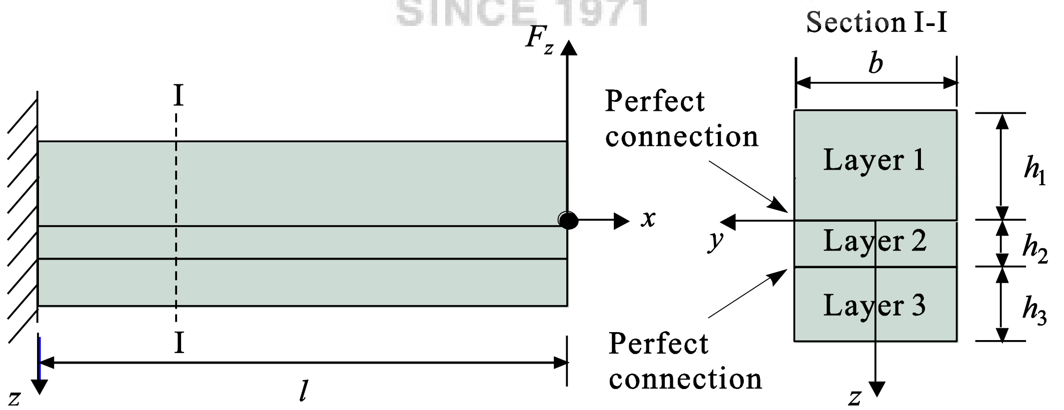

Figure 5.3(b) Three-layer perfectly connected beam subjected to tip vertical load F_z

Geometry and Loading condition	Material property
$l = 100\ \text{m}$	$E_1 = 10^5\,\text{N/m}^2$
$b = 1\text{m}$	$E_2 = 0.3\times10^5\,\text{N/m}^2$
$h_1 = 3\,\text{m}$	$E_3 = 0.7\times10^5\,\text{N/m}^2$
$h_2 = 1\,\text{m}$	$\upsilon_1 = \upsilon_2 = \upsilon_3 = 0.5$
$h_3 = 2\,\text{m}$	

Table 5.2 Geometry, material property loading condition and slip modulus for three-layer partially connected beam.

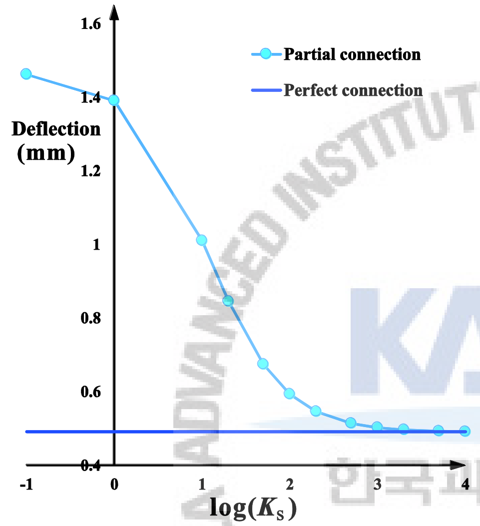

Figure 5.4(a) Deflections at the tip

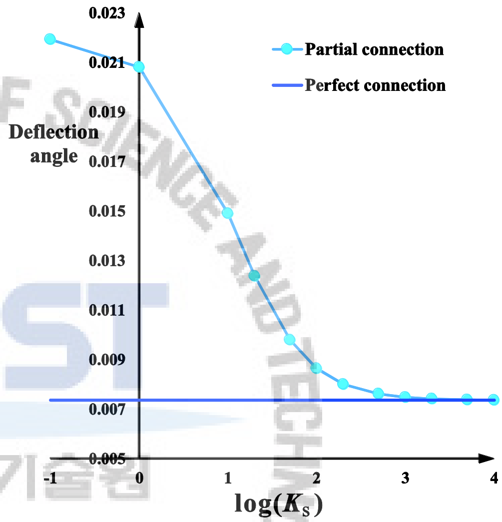

Figure 5.4(b) Deflection angles at the tip

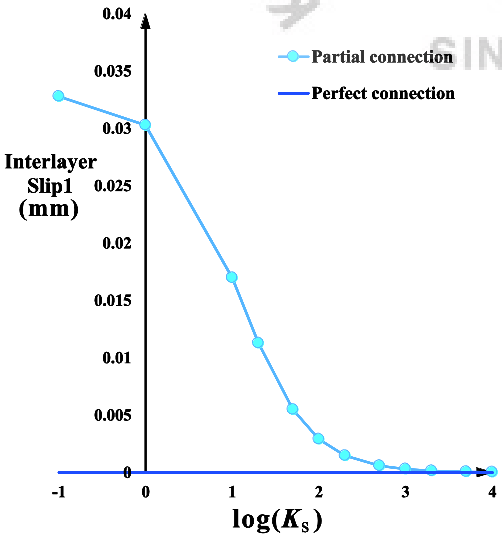

Figure 5.4(c) Interlayer slips s_1 at the tip

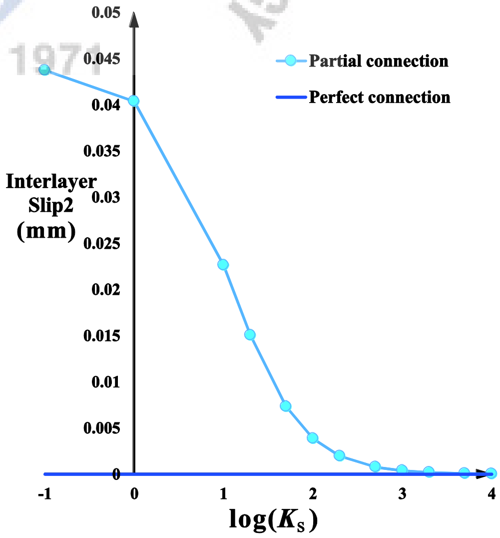

Figure 5.4(d) Interlayer slips s_2 at the tip

5.1.2 Numerical Examples

The following numerical examples demonstrate accuracy and performance of the proposed model. In order to validate and confirm the accuracy and the performance of the present beam model, the significant numerical results such as mid-point displacements and mid-point interlayer slips are compared to the reference solution found in literatures.

5.1.2.1 Two-layer Composite Beam

The first numerical example is a simply supported two-layer composite beam subjected to uniformly distributed load. The beam that considered previously by Schnabl [14], is composed of a two layers with different material property and no partial interactions ($K_s = 0$). A shear-correction factor is taken to be $6/5$ in [14]. Geometry, material properties and loading condition are shown in Figures. 5.5 and Table 5.3.

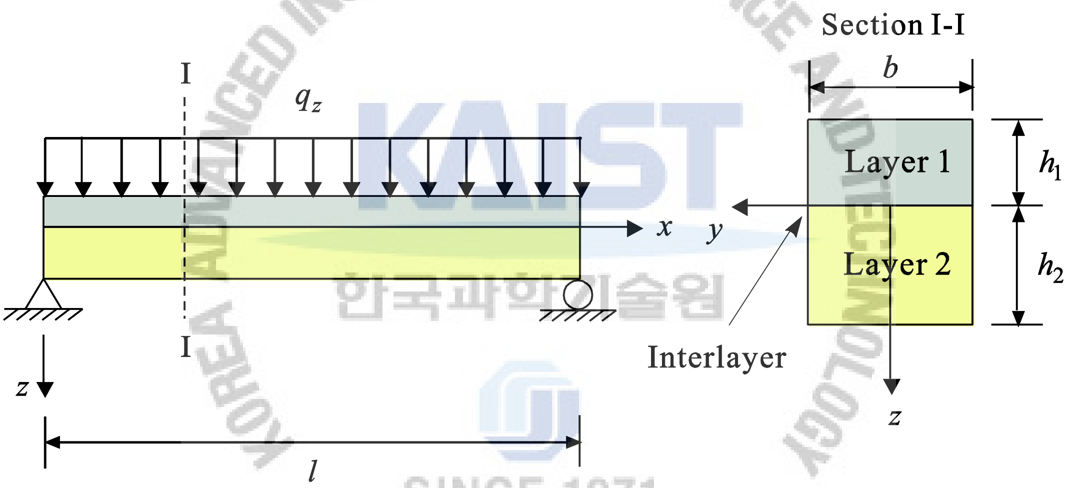

Figure 5.5 Two-layer simply supported composite beam subjected to the uniformly distributed loading with no partial interactions

Geometry and Loading condition	Material property	Slip modulus
$l = 250\,\text{cm}$	$E_1 = E_2 = 1200\,\text{kN/cm}^2$	$K_1 = 0\text{MPa}$
$b = 30\,\text{cm}$	$G_1 = 120\,\text{kN/cm}^2$	
$h_1 = 20\,\text{cm}$	$G_2 = 80\,\text{kN/cm}^2$	
$h_2 = 30\,\text{cm}$		
$q_z = 0.5\,\text{kN/cm}$		

Table 5.3 Geometry, material property loading condition and slip modulus for two-layer composite beam with no partial interaction

The rectangular cross-section of the beam is discretized by 4-node cubic cross-sectional element and $2\times2\times2$ Gauss integration is used for each cross-sectional element. The results obtained with different number of element discretization are presented in Figure 5.6(a) and Figure 5.6(b). The deflections and the interlayer slips at the mid-point of the beam are depicted along with the reference solutions obtained by [0], which is calculated by 1000 finite elements with interpolation polynomials. The numerical results of the present beam model exhibit a good agreement with the reference solutions

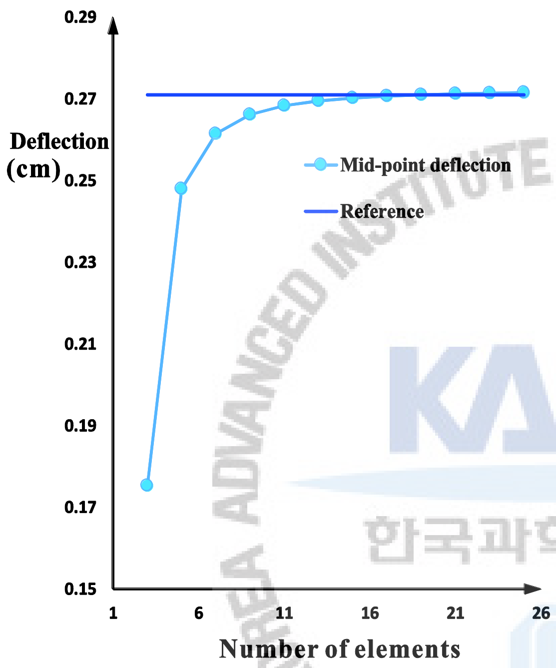

Figure 5.6(a) Deflection at the mid-point with the reference solutions

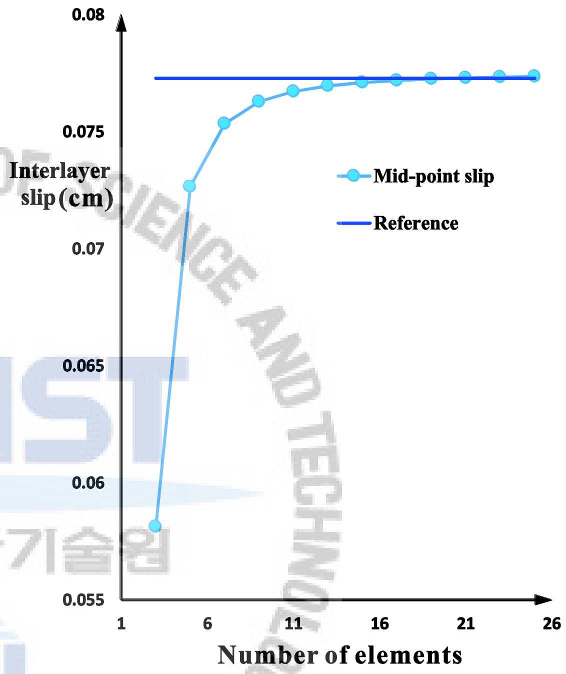

Figure 5.6(b) Interlayer slips at the mid-point with the reference solutions

5.1.2.2 Three-Layer T-Section Composite Beam

In second example, a three-layer T-section simply supported composite beam is considered as shown in Figure 5.7. The beam, referred previously by Chui and Barclay [19], is composed of three layers with different cross-section area and material properties, which is concrete topping (layer 1), a wood-based floor sheathing (layer 2) and a floor joist for (layer 3). Also, the two interlayers have different slip modulus. The z-directional concentrated load F_z is applied at the mid-span of the beam. Geometry, material property, loading condition and interface properties are summarized in Table 5.4.

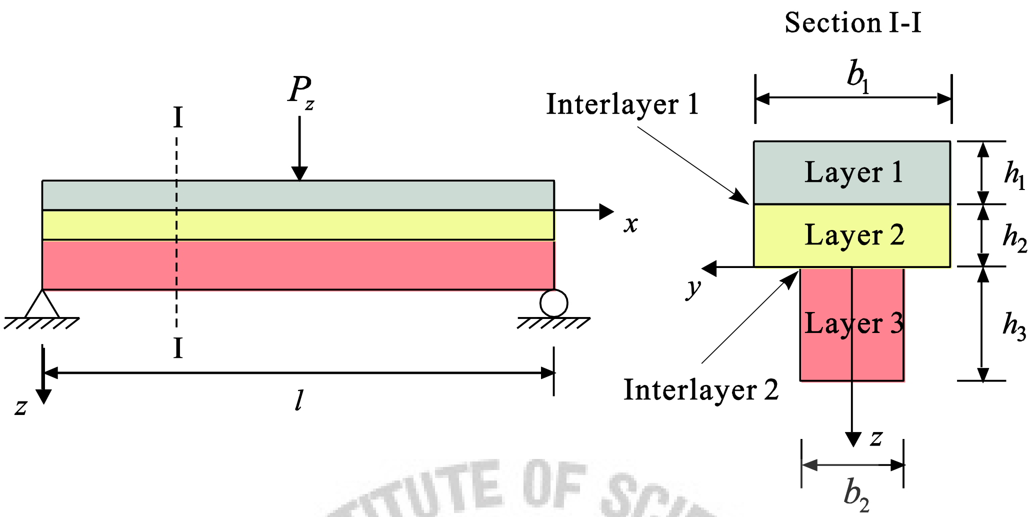

Figure 5.7 Three-layer T-section simply supported composite beam subjected to the concentrated load at mid-span

Geometry and material properties	Interface stiffness
$l = 5{,}600\,\text{mm}$	$K_1 = 11\,\text{MPa}$
$b = 150\,\text{mm}$	$K_2 = 6\,\text{MPa}$
$h_1 = 19\,\text{mm}$	
$h_2 = 9\,\text{mm}$	
$h_3 = 178\,\text{mm}$	
$b' = 40\,\text{mm}$	
$E_1 = 18{,}000\,\text{MPa}$	
$E_2 = 6{,}000\,\text{MPa}$	
$E_3 = 10{,}000\,\text{MPa}$	

Table 5.4 Geometry, material property loading condition and slip modulus for three-layer T-section composite beam.

Each rectangular cross-section layer of the beam is discretized by 4-node cubic cross-sectional element and $2\times2\times2$ Gauss integration is adopted for each cross-sectional element. The results obtained with different number of element discretization are shown in Figure 5.8. Only the deflections of the beam are discussed since there is no interlayer slip data in [2]. The deflections at the mid-point of the beam is depicted along with the reference solutions. The reference solutions in [2] are obtained by 8-node plane stress elements in ANSYS (Swanson Analysis Systems Inc. 1994) with evenly spaced 36 pairs of vertical and horizontal springs for modeling interlayer properties. As shown in Figure 5.8 the numerical results of the present beam model are in a good agreement with the reference solutions.

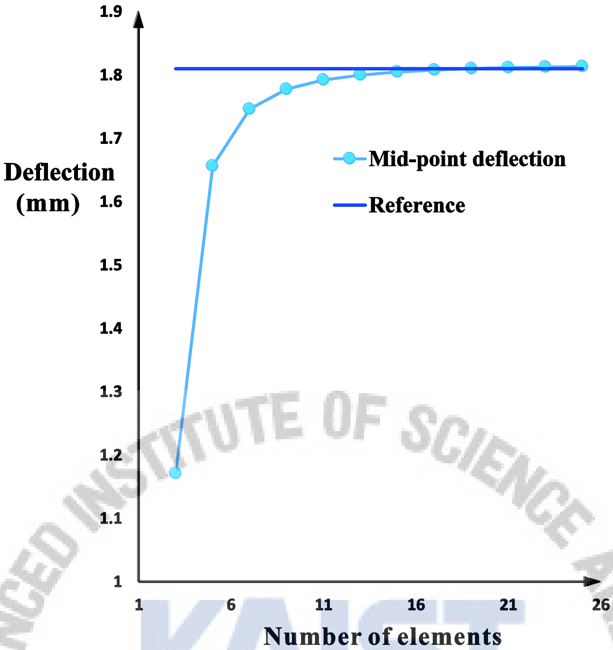

Figure 5.8 Deflections of the three-layer T-section composite beam at the mid-point along with the reference solutions

5.2 Extension to the 3D Problems

The present beam element including interlayer slips is easily extended to the three-dimensional problems with relatively small number of DOFs by applying another additional bending slip mode with bending slip DOF corresponding to extended dimension. In the present research, the three-dimensional behavior of the multi-layered composite beam is investigated

5.2.1 Six layer Three-Dimensional Composite Beam

A six-layer straight cantilever beam with rectangular cross-section shown in Figure 5.9 is considered in this example. Axial load F_x and transverse load F_y and F_z are applied to the tip of the beam. The beam is composed of three different materials and contains two interlayers in z direction and one interlayers in y direction. Therefore, three-dimensional interlayer slip displacements is observed. Geometry, material properties, loading conditions and interlayer properties are listed in Table 5.5.

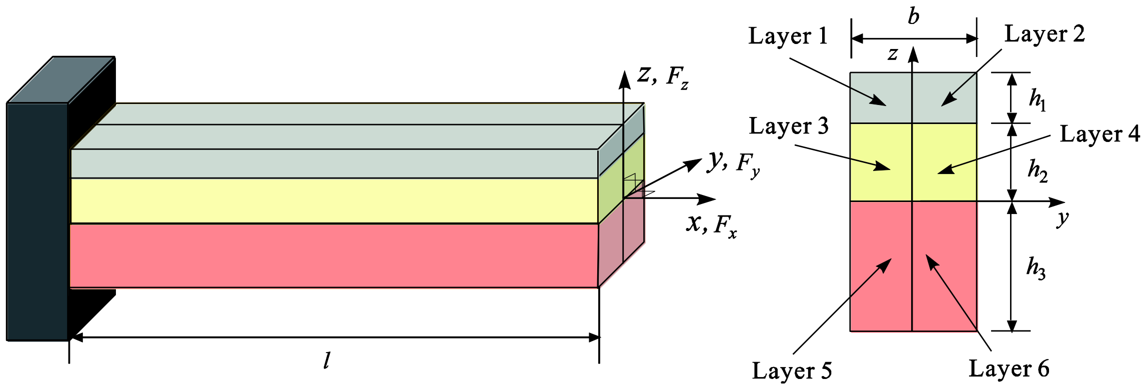

Figure 5.9 A six-layer rectangular straight cantilever beam subjected to axial load F_x and transverse load F_y and F_z.

Geometry and Loading condition	Material property	Loading condition
$l = 100\,\text{mm}$	$E_1 = 300{,}000\,\text{MPa}$	$F_x = 12000\text{N}$
$b = 2\text{mm}$	$E_2 = 20{,}000\,\text{MPa}$	$F_y = -15\text{N}$
$h_1 = 1\text{mm}$	$E_3 = 10{,}000\,\text{MPa}$	$F_z = 10\,\text{N}$
$h_2 = 2\text{mm}$	$\upsilon = 0.5$	
$h_2 = 3\text{mm}$		

Table 5.5 Geometry, material properties , loading condition and interlayer properties of the six-layer three-dimensional beam

For the analysis of the three-dimensional six-layered beam, three slip modes that are composed of one axial slip mode and two bending slip modes are employed. As a result, the displacement field of the beam is represented by 9 DOFs at each beam node k that has three translations, three rotations and three slip DOFs. The rectangular cross-section layers of the beam are discretized by 4-node cubic cross-sectional element and $2\times2\times2$ Gauss integration is adopted for each cross-sectional element.

The resulting deformed shape of the beam is depicted in Figure 5.10. As shown in Figure 5.10, interlayer slips are induced in x, y and z directions.

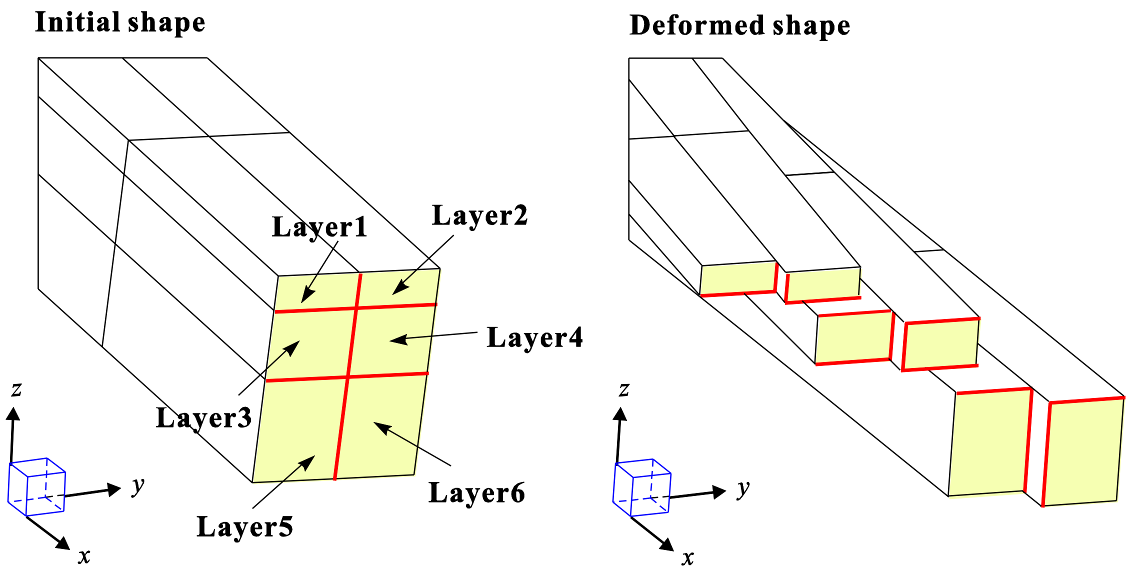

Figure 5.10 Deformed shape of the six-layer rectangular straight beam.

Also, it can be observed that the value of the interlayer slips are equivalent to the linear superposition of the two-dimensional cases in which each load is applied to the beam respectively as shown in Figure 5.11(a), Figure 5.11(b) and Figure 5.11(c). Figure 5.11(a) indicates three-layer two-dimensional beam subjected to transverse loading F_z, Figure 5.11(b) indicates two-layer two-dimensional beam subjected to transverse loading F_y and three-layer two-dimensional beam under axial loading F_x is shown in Figure 5.11(c).

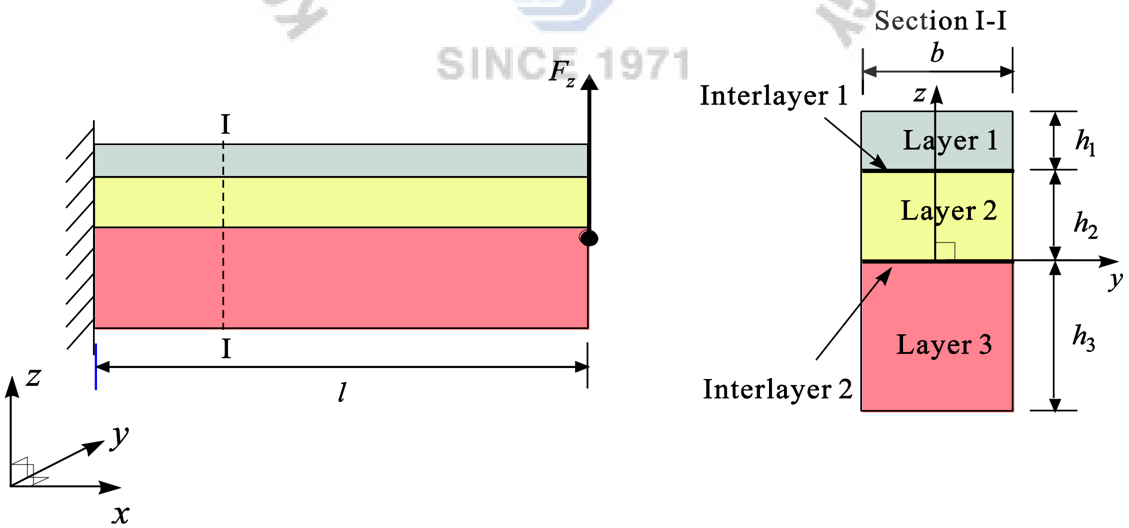

Figure 5.11(a) Three-layer two-dimensional beam subjected to transverse loading F_z

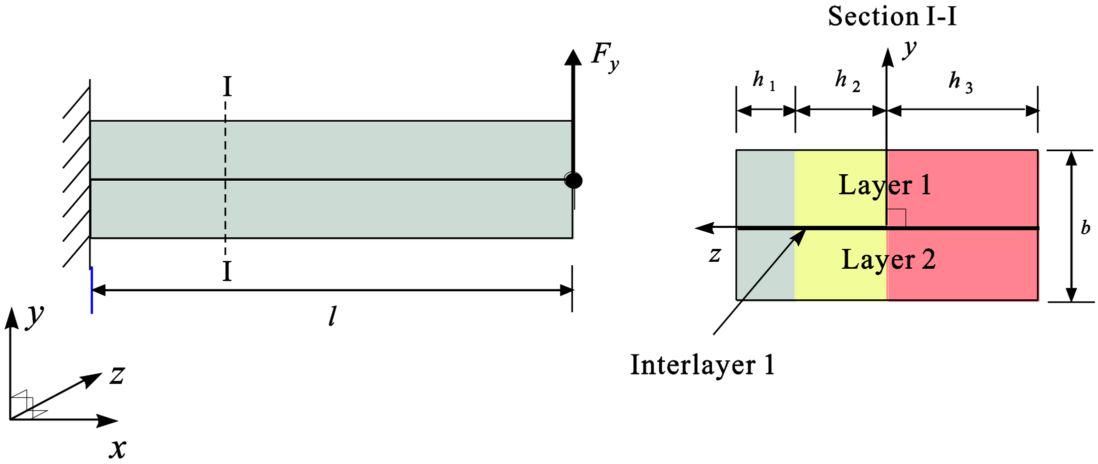

Figure 5.11(b) Two-layer two-dimensional beam subjected to transverse loading F_y

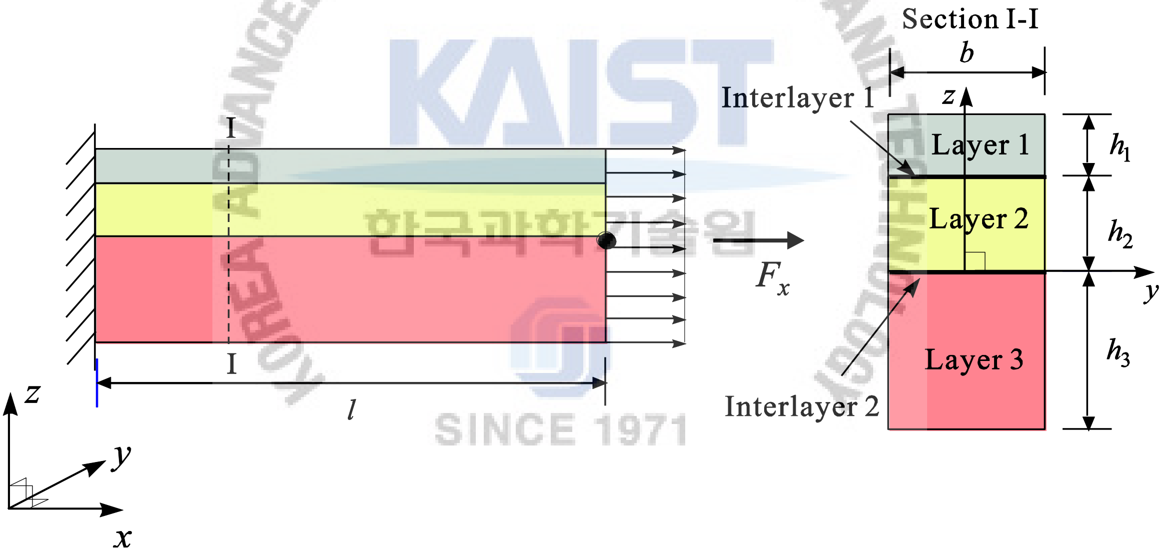

Figure 5.11(c) Three-layer two-dimensional beam under axial loading F_x

Namely, the solution of the example and deformed shape in Figure 5.10 are obtained by linear superposition of the displacements described in Figure 5.11(a), Figure 5.11(b) and Figure 5.11(c). Since the analysis is performed based on the small displacement theory, it can be concluded that the solutions are reasonable. If the beam structure undergoes large displacement exceeding their elastic limits, proper consideration of nonlinearity is required.

Chapter 6. Conclusions

6.1 Concluding Remarks

In the present research, the beam finite element which is applicable to the three-dimensional analysis of the multi-layered composite beam structures with relatively small number of DOFs was introduced. Since the total slip displacements are represented by the slip modes with the slip modulus, only two additional DOFs at each beam node are required for the two-dimensional analysis procedure and it can be easily extended to the three-dimensional problems by inserting another slip DOF corresponding to the extended dimension.

In order to verify the present beam model, several numerical studies are performed. Firstly, the present beam model is compared to the conventional one to demonstrate the influence of the slip modulus on the partial interaction effect. The results show that the solution of the partially connected beam converge to the solution of the conventional beam as slip modulus increases. Secondly, the numerical examples discussed by many other authors are examined. The two cases of two-layer rectangular composite beam with no partial interaction and three-layer T-section composite beam with deformable connections are evaluated by the comparison of the significant numerical results such as mid-point displacements and interlayer slips. The numerical results of the present beam model exhibit a good agreement with the reference solutions. Lastly, extension to three-dimensional problem is introduced.

The main advantage of the present beam model is that any multi-layered beam can be modeled by a single beam with slip modes. It means that additional procedures or interface elements for the interlayer properties are not required since slip function is calculated automatically based on the geometry and material properties of the beam. Therefore, the present beam element enables straightforward modeling of the multi-layered composite beam with relatively small number of DOFs. Also, three-dimensional analysis can be easily performed without complicated modeling, but by applying additional slip mode with corresponding slip DOF.

6.2 Further study

As an extension of the present research, the following future works need to be discussed.

- The present beam finite element including slip modes is developed based on the linear elastic behavior of the beam and load-slip relations. For more accurate analysis of the actual structure behavior, nonlinear load-slip relation and frictional effect need to be considered. Also, extension to the nonlinear formulation is worthy for future works.

- In spite of many analyses of the rectangular cross-section beam, researches about multi-layered beam with arbitrary geometry have been rarely discussed. It is expected that the concept of slip mode can be extended to the more general method applicable to the arbitrary geometry such as inclined interlayers and circular cross-section as multi-layered pipes.

- In the present model, only transverse loading and uniformly distributed axial loading are considered. For more general analysis, more general slip functions for arbitrary loading conditions need to be implemented.

References

[1] S.P. Timoshenko, J.N. Goodier, Theory of Elasticity, McGraw Hill, 1970.

[2] K.J. Bathe, Finite Element Procedures, Prentice Hall, 1996.

[3] P.S. Lee, H.C. Noh, C.K. Choi, Geometry-dependent MITC method for a 2-node iso-beam element, Struct. Eng. Mech. 29 (2008) 203-221.

[4] K. Yoon, Y.G. Lee, P.S. Lee, A continuum mechanics based beam finite element with warping displacements and its modeling capabilities. Struct. Engrg. Mech. 43 (2012) 411-437.

[5] K Yoon, P.S. Lee, Nonlinear performance of continuum mechanics based beam elements focusing on large twisting behaviors, Comput. Methods Appl. Mech. Engrg. 281 (2014) 106-130.

[6] Newmark NM, Siest CP, Viest CP. Test and analysis of composite beams with incomplete interaction. Proc Soc Exp Stress Anal 1951;9(1):75–92.

[7] Girhammar UA, Pan DH. Exact static analysis of partially composite beams and beam-columns. Int J Mech Sci 2007;49(2):239–55.

[8] Goodman JR, Popov EP. Layered beam systems with interlayer slip. J Struct Div, Proc Am Soc Civil Eng 1968;94(11):2535–47.

[9] Schnabl S, Saje M, Turk G, Planinc I. Analytical solution of two-layer beam taking into account interlayer slip and shear deformation. J Struct Eng ASCE 2007;133(6):886–95.

[10] Xu R, Wu YF. Static, dynamic and buckling analysis of partial interaction composite beams using Timoshenko's beam theory. Int J Mech Sci 2007;49: 1139–55.

[11] Ranzi G, Bradford MA, Uy B. A direct stiffness analysis of a composite beam with partial interaction. Int J Numer Methods Eng 2004;61:657–72.

[12] Battini JM, Nguyen QH, Hjiaj M. Non-linear finite element analysis of composite beams with interlayer slips. Comput Struct 2009;87:904–12.

[13] Nguyen QH, Martinelli E, Hjiaj M. Derivation of the exact stiffness matrix for a two-layer Timoshenko beam element with partial interaction. Eng Struct 2011;33:298–307.

[14] Schnabl S, Saje M, Turk G, Planinc I. Locking-free two-layer Timoshenko beam element with interlayer slip. Finite Elem Anal Des 2007;43(9):705–14.

[15] Cˇas B, Saje M, Planinc I. Non-linear finite element analysis of composite planar frames with an interlayer slip. Comput Struct 2004;82(23–26):1901–12.

[16] Sousa Jr JBM. Exact finite elements for multilayered composite beam-columns with partial interaction. Comput Struct 2013;123:48–57. doi:10.1016/j.compstruc.2013.04.008.

[17] Daví G, Milazzo A, Orlando C. An analytical solution for multilayered beams subjected to ends loads. Compos Struct 2014;116:772–81. doi:10.1016/j.compstruct.2014.06.003.

[18] Monetto I. Analytical solutions of three-layer beams with interlayer slip and step-wise linear interface law. Compos Struct 2015;120:543–51. doi:10.1016/j.compstruct.2014.09.003.

[19] Chui Y, Barclay D. Analysis of three-layer beams with non-identical layers and semi-rigid connections. Can J Civ Eng 1998:271–6.

요 약 문

3 차원 빔 해석에서의 내부 슬립 모델링

본 논문에서는 적층빔에서의 불완전한 전단 연결로 인한 휨강성의 저하와 경계면에서의 슬립을 모델링할 수 있는 빔 유한요소를 제시한다. 적층빔의 각 구성요소를 개별적으로 해석하는 방법이 아닌, 하나의 빔과 빔 절점에서의 슬립모드를 통해서 전체 적층빔을 모델링한다. 슬립모드는 빔의 단면에서 정의되는 슬립함수와 빔 절점에서의 슬립 자유도를 통해서 모델링되며, 슬립 모듈러스와 함께 경계면에서의 불완전한 전단 연결을 나타낸다. 이를 통해서 적층빔에서의 경계면의 수와 관계없이 상대적으로 적은 자유도만으로도 전체 적층빔의 모델링이 가능하다. 또한 슬립 자유도를 추가함으로써 간단히 3D 모델로의 확장이 가능하다.

핵심어: 적층빔, 슬립, 슬립 모드